

# 08 JST-3662-2022.pdf

---

WORD COUNT

12021

TIME SUBMITTED

22-MAR-2023 07:19AM

PAPER ID

97868497



## 1 **Potential of Fatty Acid Methyl Ester as Diesel Blends Produced from Free Fatty Acid in Waste Cooking Oil Catalyzed by Montmorillonite-Sulfonated Carbon**

Hasanudin Hasanudin<sup>1,2\*</sup>, Wan Ryan Asri<sup>1,2</sup>, Firda Rahmania Putri<sup>1,2</sup>, Fahma Riyanti<sup>1,2</sup>, Zainal Fanani<sup>1,2</sup>, Addy Rachmat<sup>1,2</sup>, Novia Novia<sup>3</sup> and Tuty Emilia Agustina<sup>3</sup>

6

<sup>1</sup>Department of Chemistry, Faculty of Mathematics and Natural Science, Universitas Sriwijaya, Indralaya 30662, Indonesia

<sup>2</sup>Biofuel Research Group, Laboratory of Physical Chemistry, Faculty of Mathematics and Natural Science, Universitas Sriwijaya, Indralaya 30662, Indonesia

<sup>3</sup>Department of Chemical Engineering, Department of Engineering, Universitas Sriwijaya, Indralaya 30662, Indonesia

### ABSTRACT

This research, biodiesel production from waste cooking oil (WCO), was conducted using a montmorillonite-sulfonated carbon catalyst from molasses. The biodiesel product would be blended with diesel fuel with various volume variations to see its fuel properties. The catalyst was assessed by Fourier-transform infrared spectroscopy (FTIR), scanning electron microscope (SEM), N<sub>2</sub> adsorption-desorption isotherm, and acidity analysis using the titration method. The effect of the weight ratio of montmorillonite to sulfonated carbon was also evaluated. The process of esterification reaction was optimized using

the response surface methodology with a central composite design (RSM-CCD).

The study showed that the weight ratio of montmorillonite to sulfonated carbon of 1:3 generated the highest acidity of 9.79 mmol/g with a prominent enhanced surface area and was further employed to optimize the esterification reaction. The optimum condition was obtained at a reaction temperature of 78.12°C, catalyst weight of 2.98 g, and reaction time of 118.27 with an FFA conversion of 74.101%. The optimum condition for the mixture of

### ARTICLE INFO

#### Article history:

Received: 19 May 2022

Accepted: 22 July 2022

Published: 06 March 2023

DOI: <https://doi.org/10.47836/pjst.31.2.08>

#### E-mail addressess:

hasanudin@mipa.unsri.ac.id (Hasanudin Hasanudin)  
wanryanry@gmail.com (Wan Ryan Asri)  
08031281722023@student.unsri.ac.id (Firda Rahmania Putri)  
fatechafj@unsri.ac.id (Fahma Riyanti)  
zainalf313@unsri.ac.id (Zainal Fanani)  
addy.tea@gmail.com (Addy Rachmat)  
novia@ft.unsri.ac.id (Novia Novia)  
tuty\_agustina@unsri.ac.id (Tuty Emilia Agustina)

\*Corresponding author

FAME and diesel fuel was achieved at the composition of the B20 blend, which met the FAME standard. The reusability study revealed that the catalyst had adequate stability at three consecutive runs, with a reduced performance was 18.60%. The reduction of FFA conversion was due to the leaching of the catalyst's active site. This study disclosed that the FAME generated from the esterification of FFA on WCO-catalyzed montmorillonite-sulfonated carbon had a promising option as biodiesel blends for increasing the quality of commercial diesel.

*Keywords:* Biodiesel blends, free fatty acid conversion, montmorillonite, optimization, sulfonated carbon, waste cooking oil

## INTRODUCTION

The demand for petroleum is rising in tandem with the economic and population expansion rate. Petroleum reserves are depleted due to increased oil usage in transportation and industry. Renewable and ecologically acceptable alternative energy is required to solve the energy sector's growing issues (Sari et al., 2021; Yuliana et al., 2020). It has been known that solar, wind, and bioenergy considerably contribute to the resource<sup>34</sup> of global energy production and pollution reductions. Waste resources, for example, have been employed to make biofuels, which can play an essential part in the energy sector and greatly enhance the world's socioeconomic structure (Jamil et al., 2020). Biodiesel is the potential choice among biofuels due to its low toxicity, biodegradable, carbon-neutral emissions with less sulfur, hydrocarbons, and carbon monoxide content. Biodiesel has the primary prospective to replace conventional diesel as a favorable alternative fuel in diesel engines (Chen et al., 2019).

Various raw materials for biodiesel production have been widely developed due to they are directly related to production costs. Generally, raw materials sourced from non-edible oil are much preferable to vegetable oil (Ali et al., 2018). Non-edible oil such as jatropha or castor oil can be used as raw material for biodiesel production. Even though those materials can produce biodiesel, it does not compete directly with food-grade oil and still requires a large plantation area, so their utilization becomes ineffective (Mazubert et al., 2014). In the recent development of biodiesel feedstocks, the uses of oil wastes have been massively studied due to their numerous advantages (Chen et al., 2022). Waste cooking oil (WCO), palm oil waste, animal fat, and grease, as low-cost raw materials, have been utilized for biodiesel production (Boffito et al., 2013). Currently, a large amount of waste oil is specifically generated by the food processing industry, which, unfortunately, is mostly discharged into municipal sewer systems. This condition contributes to the pollution of various areas and potentially poses a hazard to ecosystems and humans (Soegiantoro et al., 2019). This situation indicates implications for broad opportunities to use WCO as biodiesel feedstock.

WCO has high free fatty acid (FFA) content which can be used as a precursor for biodiesel (Sree et al., 2021). In the study of biodiesel production from WCO, the use of catalysts is critical and dramatically affects the effectiveness and efficiency of biodiesel production. Various types of catalysts have been employed to produce biodiesel from WCO. A homogeneous catalyst such as sulfuric acid has a high FFA conversion capability and exhibits a high biodiesel yield (Ding et al., 2012). Nonetheless, the homogeneous catalyst is corrosive and challenging to separate, generates much water due to purification, and takes up high costs (Suwannasom et al., 2016). The heterogeneous catalyst as a prominent component clearly could resolve those problems as indicated it can be separated and reused, which inherently decreases the cost of production and increases the production efficiency (Zik et al., 2020).

Currently, along with the development of science, the types of catalysts are increasingly diverse in the context of biodiesel production from WCO. The heterogeneous catalyst such as eggshells (Gupta & Rathod, 2018; Kamaronzaman et al., 2020b), bimetallic-CaO derived from eggshells (Mansir et al., 2018), bone-based catalysts (Ali et al., 2018; Suwannasom et al., 2016), sulfonated resin/PVA composite (Zhang et al., 2016), solid acid resins (Boffito et al., 2013), tailored magnetic nano-alumina (Yahya et al., 2018), Fe-montmorillonite K10 (Yahya et al., 2020), Mg/Al hydrotalcite (Munir et al., 2016), and sulfonated carbon (Kumar et al., 2020; Nata et al., 2017), have been extensively used and studied in the biodiesel production from WCO. The use of sulfonated carbon catalysts has attracted interest in biodiesel production because highly active sites result in high catalytic activity in FFA conversion (Bastos et al., 2020).

Interestingly, low-cost carbon sources are abundantly available and can be easily functionalized with sulfonate functional groups. Numerous low-cost precursors derived from biomasses have been employed as carbon precursors (Bastos et al., 2020; Farabi et al., 2019; Lathiya et al., 2018; Ngaosuwan et al., 2016; Niu et al., 2018; Rocha et al., 2019). As waste from sugar factories, Molasse has a good prospective as a source of carbon material because they have a fairly high sugar content (Palmonari et al., 2020). Carbon derived from molasses shows good physical, chemical, and absorptive properties (Kumar et al., 2020).

Hence, the carbonization of molasse potentially generated high carbon content, effectively promoting the functionalization of the sulfonated group. In order to increase the sulfonated carbon catalyst activity, it is necessary to combine with layered or porous supported materials (Munir et al., 2021). It has been reported that clay material such as montmorillonite has Bronsted and Lewis acid, which could promote high conversion and catalytic activity (Hasanudin, Asri, Tampubolon, et al., 2022; Yahya et al., 2020). Therefore, combining montmorillonite with sulfonated carbon derived from molasses potentially exhibits a synergistic effect on the FFA conversion from WCO.

Optimization of FFA conversion from WCO is crucial to getting the desired product along with improving the process feasibility and profitability (Al-Sakkari et al., 2020; Helmi et al., 2020; Sahani et al., 2020; Sharma et al., 2019; Tan et al., 2017; Sree et al., 2021). Furthermore, the simultaneous interaction of each process variable also greatly affects the magnitude of the FFA conversion (Tan et al., 2017). Response surface methodology (RSM) with central composite design (CCD) is a statistical tool that can optimize as well as evaluate the interaction of variables (Singh et al., 2018). The RSM-CCD is highly efficient for demonstrating the second-order model of experimental data and provides adequate estimation (Dhwane et al., 2015; Karmakar & Halder, 2021).

According to the literature review, there are neither studies nor explorations regarding the optimization of FFA conversion from WCO using montmorillonite-sulfonated carbon catalyst by RSM-CCD, as well as the potential of FAME produced as diesel blends. In this study, RSM-CCD was employed to determine the optimum FFA conversion derived from WCO as a response variable using a montmorillonite-sulfonated carbon catalyst. The process variables were assessed: reaction time, catalyst weight, and reaction temperature. The effect of the montmorillonite to sulfonated carbon ratio on the acidity catalyst was evaluated. The catalyst was characterized using FTIR, SEM, and N<sub>2</sub> adsorption-desorption isotherm. The reusability of the catalyst was investigated in three consecutive cycles. Moreover, to see the potential of fatty acid methyl ester (FAME) derived from WCO as diesel blends, the FAME product would be blended with diesel fuel with various volume variations to see its physicochemical properties such as water content, density, volume distillate, kinematic viscosity, and pour point, color, and cetane index.

## MATERIALS AND METHODS

### Preparation of Catalyst

Briefly, 200-mesh of natural montmorillonite was washed using demineralized water and dried at 120°C for 24 hours in the oven. Next, various weight ratios of montmorillonite to molasses were dissolved in 500 ml of demineralized water, namely 3:1, 2:1, 1:1, 1:2, 1:3, 1:4 (% w/w), and stirred for 1 hour at 80°C. The mixture was later dried in the oven at 120°C. According to Suganuma et al. (2012), the carbonization was conducted with some modifications by employing a temperature of 400°C for 15 hours in the N<sub>2</sub> atmosphere. The powder was referred to as montmorillonite-carbon composites. The sulfonation was conducted using 20 g of the montmorillonite-carbon composite and mixed with 100 ml of concentrated H<sub>2</sub>SO<sub>4</sub> in the reflux system at 175°C for 15 hours. After that, the powder was washed with hot water until the pH was close to neutral, followed by centrifugation, and dried for one day at 120°C. The powder was referred to as montmorillonite-sulfonated carbon composite. The acidity of the catalyst was determined using the titration method. The catalyst morphology and its elemental content were assessed using SEM (JEOL), whereas

the functional group catalyst was characterized using FT-IR (Shimadzu). The textural properties were characterized using N<sub>2</sub> adsorption-desorption isotherm (Quantachrome NOVA)

### Esterification of FFA from WCO

The esterification was conducted under a reflux system. 25 g of WCO was mixed with 79 ml of methanol, followed by the montmorillonite-sulfonated carbon composite catalyst from molasses. The esterification product was separated from the catalyst. Subsequently, 50 mL of distilled water was added and allowed to stand until two layers, such as FAME and glycerol, were formed. The FAME was distilled to remove the alcohol and water. The product was characterized using FTIR. The FFA content was analyzed using the titration method with NaOH. The FFA conversion (X) was calculated according to Equation 1:

$$X (\text{wt}\%) = \frac{F_0 - F}{F_0} \quad (1)$$

Where F<sub>0</sub> and F are the FFA content of feedstock and the esterification product, respectively.

### Experimental Design

This study consisted of 17 run experiments to investigate the optimum interaction and conditions in the conversion of FFA from WCO. The design of the experiment using CCD is shown in Table 1. The quadratic model is shown in Equation 2:

$$Y = \alpha_0 + \sum_{i=1}^n \alpha_i X_i + \sum_{i=1}^n \alpha_{ii} X_i^2 + \sum_{i=1}^{n-1} \sum_{j=i+1}^n \alpha_{ij} X_i X_j \quad (2)$$

Here Y is the response (FFA conversion), α<sub>0</sub> is the constant coefficient, whereas α<sub>i</sub>, α<sub>ii</sub>, and α<sub>ij</sub> are the coefficients for linear, quadratic, and interaction effects, respectively, and X<sub>j</sub> are the process variables (Anguebes-Franceschi et al., 2018). The model's fit was evaluated using analysis of variance (ANOVA).

Table 1

The levels of process variables using CCP

| Process variable         | Unit | Levels |    |     |     |        |
|--------------------------|------|--------|----|-----|-----|--------|
|                          |      | -1.628 | -1 | 0   | +1  | +1.628 |
| Reaction temperature (A) | °C   | 63.18  | 70 | 80  | 90  | 96.82  |
| Catalyst weight (B)      | g    | 0.31   | 1  | 2   | 3   | 3.68   |
| Reaction time (C)        | min  | 69.55  | 90 | 120 | 150 | 170.45 |

### Catalyst Reusability

Regarding the catalyst reusability study, the spent catalyst after the esterification reaction was vacuum filtered and washed with alcohol four times. The catalyst was later dried and stored for employment in the next cycle of esterification at optimum conditions.

### FAME and Diesel Blend Composition

The FAME produced from the highest FFA conversion was blended with diesel fuel with various compositions (Table 2). The sample was shaken for 10 minutes and then allowed to stand for one hour at room temperature.

Table 2  
*Blend composition of FAME and diesel fuel*

| Product | FAME |    | Diesel fuel |     |
|---------|------|----|-------------|-----|
|         | %    | mL | %           | mL  |
| B5      | 5    | 20 | 95          | 380 |
| B10     | 10   | 20 | 90          | 360 |
| B15     | 15   | 60 | 85          | 340 |
| B20     | 20   | 80 | 80          | 320 |

### FAME Characterization

The FAME, diesel, and blended water content were analyzed according to ASTM D6304 using the Karl Fischer method. The density was analyzed according to ASTM 41298 using a hydrometer. ASTM D86 was used to evaluate the distillation volume of fuel. The kinematic viscosity was determined according to ASTM D445. The color of the fuel was analyzed using ASTM D1500. Furthermore, the standard of ASTM D97 and ASTM D4737 was used to evaluate the fuel's pour point and cetane index, respectively. The FAME product was compared to the European FAME standard (EN 14214:2012). The functional groups of FAME were also assessed using FTIR.

## RESULTS AND DISCUSSION

### Catalyst Characterization

The montmorillonite-sulfonated carbon catalyst was characterized using FT-IR, SEM, and acidity. Figure 1 shows the FT-IR spectra of the catalyst with a variation ratio of montmorillonite to sulfonated carbon of 1:3, 1:1, and 3:1 (% w/w). The absorption peaks at  $1087.05\text{ cm}^{-1}$  and  $779.23\text{ cm}^{-1}$  were attributed to the interaction of Si-O-Si

and Si-<sub>2</sub>Al bonds from montmorillonite (Munir et al., 2021). The absorption band at 3424.2 cm<sup>-1</sup> indicated stretching vibrations [10] the hydroxyl groups. Subsequently, the functional groups of C=C and C-H aromatic were observed at 1628.28 cm<sup>-1</sup> and 665.26 cm<sup>-1</sup> due to [the] carbonization of molasses, which formed a polycyclic aromatic carbon [18] npound, respectively (Flores et al., 2019). All peaks appeared in all catalyst variations. The absorption band at 1082 cm<sup>-1</sup> corresponded [47] the -SO<sub>3</sub>H functional group due to the sulfonation process (Fadhil et al., 2016), whereas the absorption band at 452 cm<sup>-1</sup> indicated the C-S-C bond (Fauziyah et al., 2020). Furthermore, Figure 1 shows that the sulfonated group intensity gradually increased as the carbon ratio increased. The more molasses composition, thus the more molasses is converted into carbon. This carbon framework could support the catalyst's active site (Tang et al., 2020). Hence, more SO<sub>3</sub>H group was functionalized in the polycyclic aromatic carbon.

The effect of [62] montmorillonite to sulfonated carbon (% w/w) ratio on the acidity of the catalyst is shown in Figure 2. The acidity increased along with the increase in carbon composition. The highly volatile components of molasses are released during the carbonization process [70] leaving catalyst support with a high carbon content that provides the functionalization of the -SO<sub>3</sub>H active site during the sulfonation process (Endut et al., 2017). As molasses weight composition increased, the [76] pon formation also increased; consequently, a more sulfonated group was effectively attached to the carbon structure. The highest acidity of the catalyst (9.79 mmol/g) was obtained at the montmorillonite to sulfonated carbon 1:3 ratio. This finding was consistent with the FTIR analysis. The H<sup>+</sup> provided by the heterogeneous acid catalyst, the -SO<sub>3</sub>H group, was considered the active site, wherein the acidity was positively correlated to the catalytic activity (Xincheng et al., 2019). The sulfonated groups act as a Bronsted acid which could catalyze the esterification of FFA (Bastos et al., 2020). However, a prolonged high-weight ratio of montmorillonite to sulfonated carbon generated a relatively constant catalyst acidity (9.75 mmol/g) because the sulfonation process had already saturated, whereby the hydroxyl group's present in the carbon framework had been sulfonated and reached a maximum so that the acidity of the catalyst tends to remain constant.

The morphology surfaces of montmorillonite and montmorillonite-carbon sulfonated carbon catalyst is shown in Figure 3. Platy particles consisting of stacks of the layered thin structure were observed in Figure 3a. Alshabanat et al. (2013) reported that the typical montmorillonite structure was irregularly shaped and had many sides. Other studies reported similar findings (Munir et al., 2021). The composite of montmorillonite-sulfonated carbon revealed a significant morphological surface change with porous structure due to carbonization followed by sulfonation (Figure 3a). The carbonization process of molasses into carbon increases the number of cavities and pores. This condition increases the contact area over the sulfonated group, enhances the diffusion of alcohol, and promotes efficient interaction of FFA towards the active site (Fonseca et al., 2020).

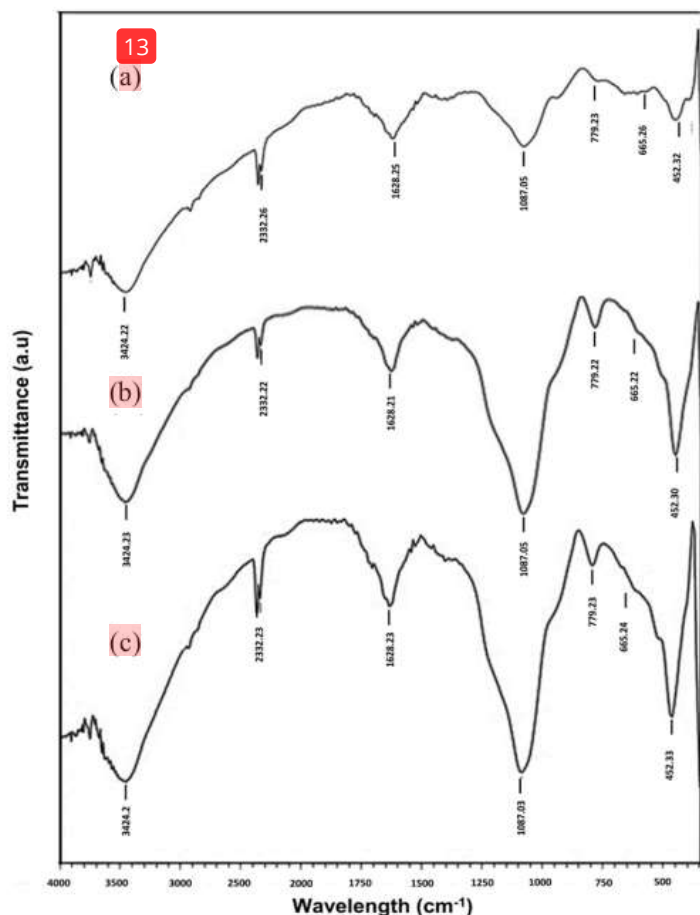
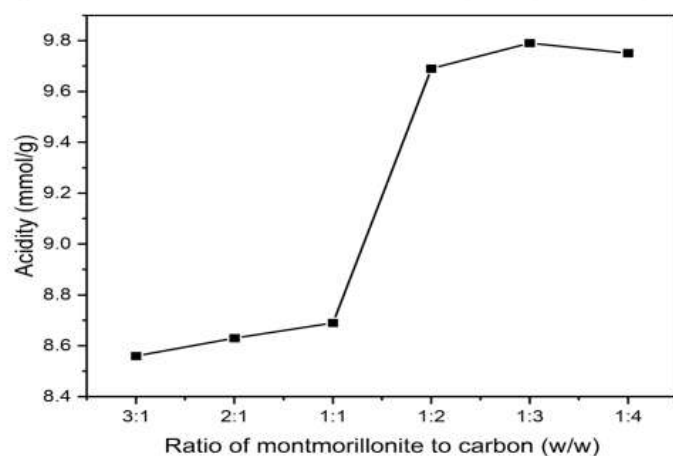


Figure 1. FTIR spectra of montmorillonite-sulfonated carbon of (a) 3:1 (b) 1:1 and (c) 1:3 catalyst



69  
Figure 2. Effect of ratio of montmorillonite to carbon (% w/w) on catalyst acidity

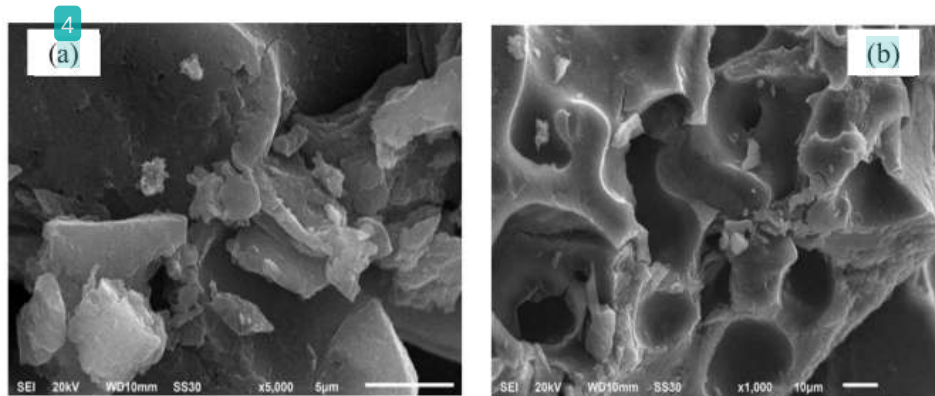


Figure 3. SEM images of (a) montmorillonite and (b) montmorillonite-sulfonated carbon catalyst

Figure 4 shows the  $N_2$  adsorption-desorption of montmorillonite and montmorillonite-sulfonated carbon catalysts. Montmorillonite and montmorillonite-sulfonated carbon revealed type IV isotherm, which had a wide pore distribution (Rabie et al., 2018). Another study reported a similar finding (Lin et al., 2018). It also can be noticed that all catalysts had an H4 hysteresis that corresponded to the aggregates of laminar, which was nearly associated with the layer structure of bentonite (Amaya et al. 2020). Moreover, The typical adsorption-desorption curve at a relative pressure ( $\sim 0.45$ ) was attributed to the existence of small mesopores on the catalyst (de Oliveira et al., 2019). This small mesopore could promote the high accessibility of the active site.  $N_2$  adsorption-desorption isotherm in Figure 4b revealed a distinctive curve at high relative pressure compared with montmorillonite, and this condition occurred presumably due to the sulfonated carbon effect. This curve was consistent with Lathiya et al. (2018), which utilized the sulfonated carbon catalyst derived from the waste orange 95 for esterifying corn acid oil.

Table 3 represents the textural properties of montmorillonite and montmorillonite-sulfonated carbon. The montmorillonite-sulfonated carbon catalyst exhibited high surface area than montmorillonite. The montmorillonite was introduced to the sulfonated carbon, thereby increasing the surface area<sup>89</sup>. High surface area promoted the extent of the functional group (-SO<sub>3</sub>H) to occupy the catalyst surface<sup>36</sup> (Rabie et al., 2019). Furthermore, the increase in surface area was might presumably due to the repulsion force between SO<sub>3</sub>H and other groups induced on the catalyst surface (Rahimzadeh et al., 2018).

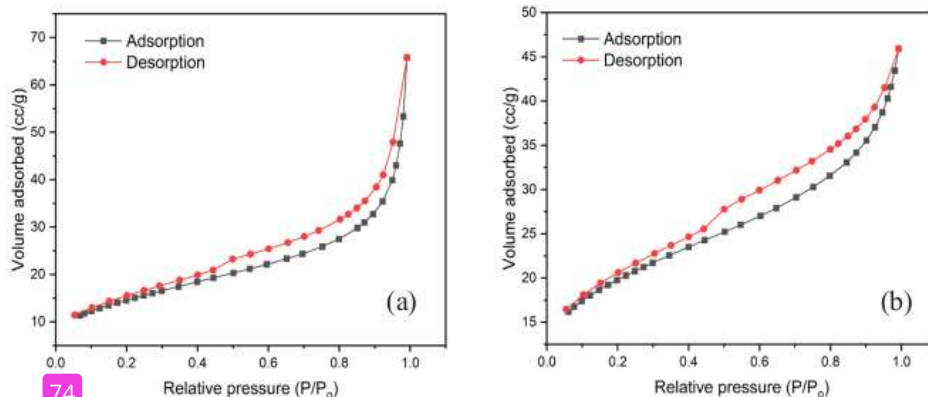


Figure 4.  $\text{N}_2$  adsorption-desorption of (a) montmorillonite and (b) montmorillonite-sulfonated carbon catalyst

Table 3

Surface area, total pore volume, and average pore radius of catalysts

| Catalyst                          | Surface area<br>( $\text{m}^2/\text{g}$ ) | Total pore volume<br>( $\text{cc}/\text{g}$ ) | Average pore radius<br>( $\text{\AA}$ ) |
|-----------------------------------|---|---|---|
| Montmorillonite                   | 52.06                                     | 0.11  | 39.09                                   |
| Montmorillonite-sulfonated carbon | 67.12                                     | 0.071   | 21.16                                   |

### Model Development and ANOVA

In this study, the montmorillonite-sulfonated carbon with a ratio of 1:3 was used for optimization because it showed the highest acidity catalyst. The relationship between the response, namely the conversion of FFA, and the process variables, namely reaction temperature, catalyst, and reaction time, were investigated. The experimental design results for 17 runs based on CCD are shown in Table 4. Substantial results were observed in the conversion of FFA under different mild conditions. FFA conversions obtained ranged from 45 to 74.29 %.

Table 4

Experimental result of FFA conversion using CCD

| Run | Reaction temperature ( $^{\circ}\text{C}$ ) | Catalyst weight (g) | Reaction time (min) | FFA conversion (%) |
|-----|---|---------------------|---------------------|--------------------|
| 1   | 70  | 1                   | 90                  | 45                 |
| 2   | 90  | 1                   | 90                  | 49.821             |
| 3   | 70  | 3                   | 90                  | 54.214             |
| 4   | 90  | 3                   | 90                  | 64.286             |

Table 4 (Continue)

| Run | Reaction temperature (°C) | Catalyst weight (g) | Reaction time (min) | FFA conversion (%) |
|-----|---------------------------|---------------------|---------------------|--------------------|
| 5   | 70                        | 1                   | 150                 | 47.321             |
| 6   | 90                        | 1                   | 150                 | 56.25              |
| 7   | 70                        | 3                   | 150                 | 73.214             |
| 8   | 90                        | 3                   | 150                 | 74.286             |
| 9   | 63.18                     | 2                   | 120                 | 44.286             |
| 10  | 96.82                     | 2                   | 120                 | 50.179             |
| 11  | 80                        | 0.31                | 120                 | 47.679             |
| 12  | 80                        | 3.68                | 120                 | 73.75              |
| 13  | 80                        | 2                   | 69.55               | 52.679             |
| 14  | 80                        | 2                   | 170.45              | 55.464             |
| 15  | 80                        | 2                   | 120                 | 65.964             |
| 16  | 80                        | 2                   | 120                 | 65.321             |
| 17  | 80                        | 2                   | 120                 | 65.179             |

The quadratic model for the conversion of FFA in the coded form is shown in Equation 3:

$$Y = 65.18 + 2.55A + 8.16B + 3.11C - 0.32AB - 0.61AC + 2.53BC - 5.40A^2 - 0.63B^2 - 2.98C^2 \quad (3)$$

The terms A, B, and C represented the single effect regarding the reaction temperature, catalyst, and reaction time, respectively (Eq 73). AB, AC, and BC represented the interaction effect for each variable, whereas the terms  $A^2$ ,  $B^2$ , and  $C^2$  were the quadratic effects. The positive and negative signs correspond to the synergistic and antagonistic effects on the FFA conversion, respectively (Almadani et al., 2018). The ANOVA of the model (95% confidence level) derived from Equation 3 is shown in Table 5.

The P-value of the model was 0.0060, which indicates that the model was statistically significant (Table 5). Likewise, the model's F-value correlated to the FFA conversion was 8.01. This F-value explained that the model was significant, and there was only a 0.60% chance that this high F-value could occur owing to noise (Balajii & Niju, 2021). Subsequently, the terms B, C, and  $A^2$  showed a P-value of <0.05, which indicated that the terms were statistically significant. Furthermore, a sufficient adequate precision value was observed to be more than 4, which was 9.3020. This condition indicated that the model generated an adequate signal and could navigate the quadratic model design (Boey et al., 2013). The statistical diagnostic was conducted to understand the development of the model.

(Figure 5). The normal plot (Figure 5a) revealed a straight line that expressed a decent direct agreement between normal probability (%) and externally studentized residuals (Hasanudin, Asri, Said et al., 2022). It appeared that the response transformation was not required and that there were no major problems with the data's normality (Chandane et al., 2020).

The residual plot (Figure 5b) showed that the data were random scattered, indicating that the proposed model accurately described the process (Helmi et al., 2020). Figure 5c shows the plot of the predicted value obtained from the quadratic model with respect to experimental value. The predicted value based on the model calculation was close to the experimental data, with the coefficient of determination ( $R^2$ ) value found to be 0.9115. This  $R^2$  value indicated that the prediction model was sufficiently accurate to identify the optimal process parameters with a response variability of 91% (Balajii & Niju, 2022). Figure 5d shows the externally studentized residual respect with a run number plot. The outliers from the run experiments showed that all residual points were in the +3.8 and -3.8 intervals, indicating a good distribution for the CCD design (Noshadi et al., 2012). The leverage respect with a run number plot is shown in Figure 5e. According to the plot, all points are less than one, which was associated with no significant error that could affect the model. Furthermore, the parameter of Cook's distance in Figure 5f revealed that all the points were under the expected, which attributed that there was no significant error in observation (Kusumaningtyas et al., 2021). All statistical diagnostics indicated that the proposed quadratic model was proficient in optimizing the FFA conversion using montmorillonite-sulfonated carbon from a molasses catalyst.

Table 5  
*ANOVA for the quadratic model*

| Source                 | Sum of square | df | Mean   | F-value  | P-value |             |
|------------------------|---------------|----|--------|----------|---------|-------------|
| Model                  | 1559.27       | 9  | 173.25 | 8.01     | 0.0060  | significant |
| A-Reaction temperature | 88.70         | 1  | 88.70  | 4.10     | 0.0825  |             |
| B-Catalyst weight      | 909.58        | 1  | 909.58 | 42.07    | 0.0003  |             |
| C-Reaction time        | 131.85        | 1  | 131.85 | 6.10     | 0.0429  |             |
| AB                     | 0.8489        | 1  | 0.8489 | 0.0393   | 0.8486  |             |
| AC                     | 2.99          | 1  | 2.99   | 0.1384   | 0.7209  |             |
| BC                     | 51.26         | 1  | 51.26  | 2.37     | 0.1675  |             |
| $A^2$                  | 328.99        | 1  | 328.99 | 15.22    | 0.0059  |             |
| $B^2$                  | 4.55          | 1  | 4.55   | 0.2106   | 0.6602  |             |
| $C^2$                  | 100.39        | 1  | 100.39 | 4.64     | 0.0681  |             |
| Residual               | 151.34        | 7  | 21.62  |          |         |             |
| Lack of Fit            | 150.99        | 5  | 30.20  | 172.5821 | 0.0058  |             |
| Pure Error             | 0.3499        | 2  | 0.1750 |          |         |             |
| Cor Total              | 1710.61       | 16 |        |          |         |             |

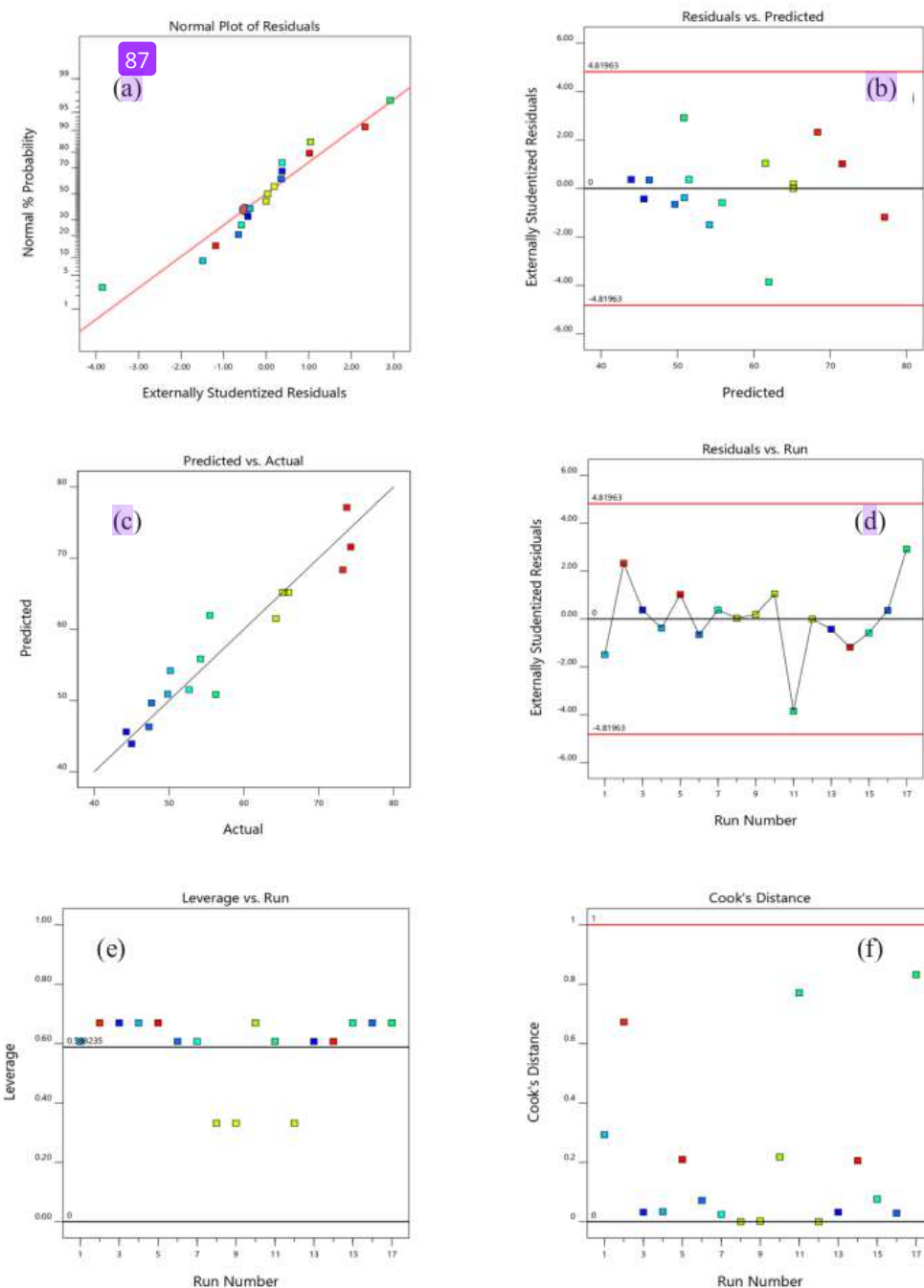
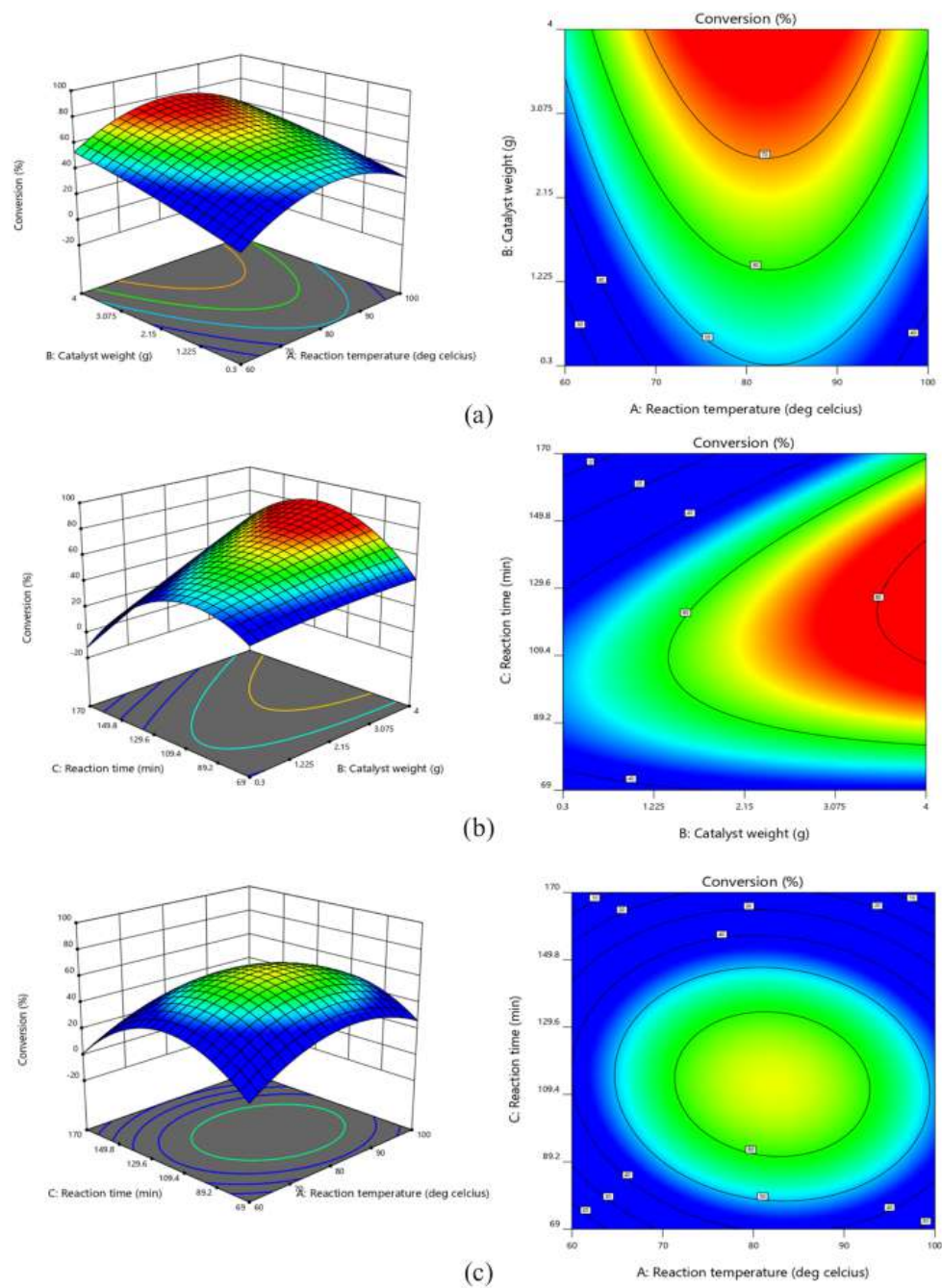


Figure 5. The statistical diagnostic of the development model

### Optimization Study

Graphical and numerical optimization<sup>8</sup> procedures were used to predict the optimum conditions of three factors, including reaction temperature, catalyst weight, and reaction time<sup>37</sup>, which resulted in the desired goal of the response variable, namely FFA conversion. The response surface and contour plots were assessed to see the interaction of variables (Figure 6). The interaction effect of a catalyst weight and a reaction temperature at a constant reaction time of 120 min is shown in Figure 6a. The highest FFA conversion was achieved up to 70% when the catalyst weight was higher than 3 g, and the reaction temperature ranged from 70–90°C. Under these conditions, a high catalyst weight presumably increased the number of active catalyst sites, promoting the high FFA conversion (Anguebes-Franceschi et al., 2018). As the temperature increased to 90°C, the collisions between reactants also increased, sufficiently leading to high FFA conversion. Furthermore, these conditions also tended to reduce the mixture's<sup>88</sup> viscosity, thereby increasing diffusion through the pores (Mulay & Rathod, 2021). Gan et al.<sup>8</sup> (2012) reported that the highest conversion of FFA in WCO was achieved up to 60.2% at a temperature of 65°C and a concentration catalyst of 4 wt.% using Amberlyst-15 catalyst. Özbay et al. (2008) used a series of ion-exchange resins, such as an Amberlyst-based catalyst. They showed that the FFA conversion was achieved up to 45.7% when the temperature was 59°C with 2% wt catalyst concentration. Sulfonated nanomagnetic biochar derived from oil palm empty fruit bunch was employed by Jenie et al. (2020), which revealed that at 2.5%wt catalyst concentration, the oleic acid conversion was exhibited up to 71.2%. The montmorillonite-sulfonated carbon derived from the molasse catalyst was likely promising in catalyzing the FFA esterification in WCO relative to previously reported catalysts.<sup>3</sup>

The interaction effect of reaction time and catalyst weight at a constant reaction temperature of 80°C is presented in Figure 6b. The FFA conversion increased at a high catalyst loading<sup>60</sup> of more than 2 g and reaction time ranged from 90–20 min. The longer reaction time did not result in a substantial increase in the FFA conversion. The reaction would approach equilibrium; therefore, no additional conversion would be generated. Jenie et al. (2020) stated that the considerable drop in conversion<sup>32</sup> longer reaction periods could be attributed to by-product generation or deactivation of the catalyst's active sites. Suresh et al. (2017) utilized sulfonated polystyrene (PSS) for esterification of FFA in WCO and reported that at a reaction temperature of 58°C and PSS concentration of 2% w/w, the conversion exhibited up to 80.8 %. Zhang et al. (2015) used sulfonated mesoporous carbon for the esterification of FFA and showed that a prolonged reaction time of up to three hours would produce high FFA conversion than 80%, whereas Dawodu et al. (2014) generated high FFA conversion derived from sludge palm oil at 4 hours reaction when employing sulfonated carbon from glucose with *C. inophyllum* seed cake.



14

Figure 6. The 3D surface and contour plot of interaction variables on the FFA conversion

3

The interaction effect of reaction time and reaction temperature at a constant catalyst weight of 2 g is shown in Figure 6c. It was found that the highest FFA conversion was achieved up to 60% at a reaction temperature of 70–90°C and a reaction time of 90–130 min. When the reaction temperature was too high, it would encourage the reverse reaction, decreasing FFA conversion. Simultaneously, the high temperature accelerates the methanol loss rate, potentially reducing catalytic effectiveness (Zhang et al., 2021). As reaction time gradually increased, the FFA conversion also increased due to the availability of sufficient time to complete the reaction (Figure 6c). However, the FFA conversion began to decrease at a long reaction time due to the reverse reaction. These results are also in accordance with the previous report (Narula et al., 2017). Furthermore, a higher reaction time was unfavorable for the esterification reaction since it consumes more energy (Fawaz et al., 2020) [53]

The optimization of FFA conversion by Design-Expert using the numerical method was used to optimize the studied parameters. According to the optimization, the optimum condition was obtained at a reaction temperature of 78.12°C, catalyst weight of 2.98 g, and reaction time of 118.27 with an FFA conversion of 74.101%. In addition, the desirability function was found to be one, which indicated that the developed solution was good. The validation showed that the predicted response was in good accordance with the experimental results.

12

## Catalyst Reusability

The study of catalyst reusability was conducted under the optimized condition obtained from RSM-CCD. Figure 7 represents montmorillonite-sulfonated carbon's reusability performance in FFA conversion at three consecutive runs. It can be noticed that the FFA conversion was slightly decreased in the first cycle. In this first cycle, 70.25% of FFA conversion was achieved, indicating a decrease in the catalyst performance up to 5.07% relative to the fresh catalyst (74% FFA conversion). Moreover, the catalyst's performance was shown significantly reduced up to 9.55% in the second cycle and noticeably decreased in the three consecutive runs, which only generated 60.23% FFA conversion. The decrease in FFA conversion could presumably be due to the active site's leaching, i.e., the sulfonate group (Dhawane et al., 2016). Another study consistently reported a similar finding (Farabi et al., 2019; Tang et al., 2020). This leaching was likely due to insufficient and ineffective regeneration through the alcohol-washing process (Ngaosuwan et al., 2016). In this regard, catalyst regeneration by performing a sulfonation process on the spent catalyst was necessary to return the catalytic activity.

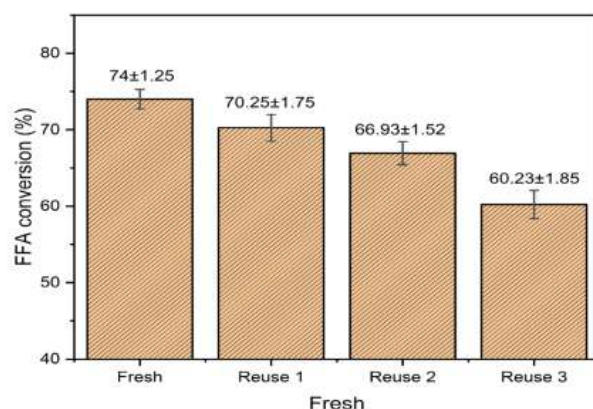
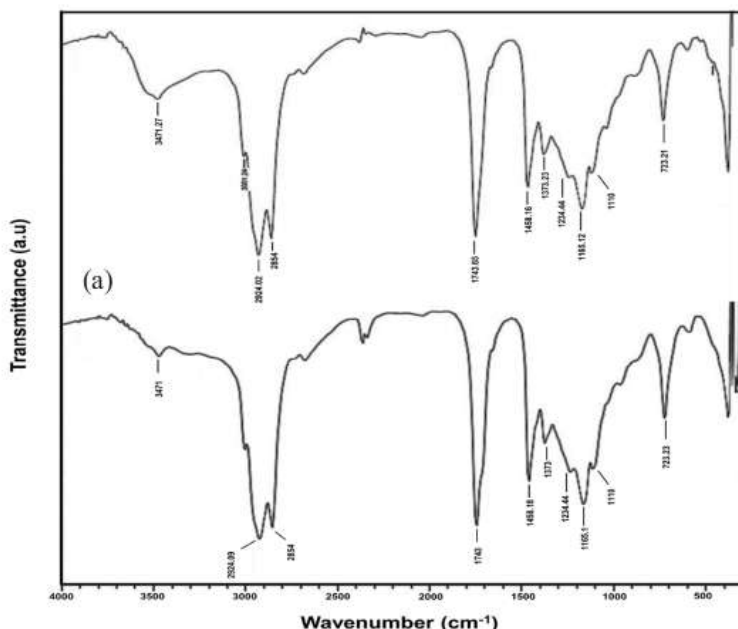


Figure 7. Reusability of catalyst

### FAME Physicochemical Properties

The FAME product generated from the optimized esterification reaction and the feedstock, namely WCO, were analyzed using GC and FTIR. GC analysis showed that WCO contained the highest fatty acid composition, namely oleic acid at 43.51% and palmitic acid at 39.75%. This finding was similar to Azman et al. (2021), which reported that WCO consisted of oleic acid (48.1%) as the primary fatty acid, followed by palmitic acid (22%). In contrast, Kumar et al. (2020) found that the WCO consisted of 46.32 wt% palmitic acid and 41.65% oleic acid. These different results are due to the diversity of waste cooking oil sources. The analysis results of FFA content in WCO using the titration method were 36.94%. The FFA content on WCO decreased to 5.938% after esterification using montmorillonite-sulfonated carbon catalyst with a conversion of 83.925%, which indicated that FFA from WCO was potential as a FAME feedstock. In this reaction, the sulfonated groups on the montmorillonite framework act as an active site of Bronsted acid, which could catalyze the esterification of FFA from WCO (Hasanudin, Putri, et al., 2022). The FTIR of WCO and the product of esterification are presented in Figure 8. It can be seen that due to the main structural change was the substitution of methanol in the hydrocarbon chain, the FTIR spectrum of FAME was mainly similar to the WCO, as consistent with previous reports (Kamaronzaman et al., 2020a; Rafati et al., 2019).

The absorption bands from Figure 8a at  $2924.02\text{ cm}^{-1}$  and  $164\text{ cm}^{-1}$  were attributed to C-H symmetrical and asymmetrical alkane groups (Banerjee et al., 2019). Subsequently, 54 absorption bands at  $1743.65\text{ cm}^{-1}$  corresponded to the ester groups from triglyceride. Furthermore, the region bands at  $1458.16\text{ cm}^{-1}$  and  $1373.23\text{ cm}^{-1}$  indicated the C-H bending vibration (Mahesh et al., 2015), also revealed in Figure 8b. FAME provided a strong absorption band due to the vibrations of the C=O and C-O bonds. The absorption band at



79  
Figure 8. FTIR spectra of (a) WCO and (b) Esterification product

1743.65  $\text{cm}^{-1}$  was commonly from the C=O carbonyl group in saturated aliphatic esters (Helmi et al., 2020). The aryl and  $\alpha,\beta$ -unsaturated structures could generate a minor shift in these bands to lower wavenumber (Omidvarborna et al., 2016).

Subsequently, the C-O stretching vibrations appeared at a broader range at 1110  $\text{cm}^{-1}$  and were also observed in the FAME spectrum. Long-chain fatty acids in FAME often exhibited an increment to maximum absorption approximately at the absorption band at 1234.44  $\text{cm}^{-1}$ , 1165  $\text{cm}^{-1}$ , and 723.23  $\text{cm}^{-1}$ , respectively (Bahú et al., 2017; Wu et al., 2015). The absorption band at 3471  $\text{cm}^{-1}$  indicated the hydroxyl group vibration absorbed by the catalyst (Akram et al., 2019).

The results of the FAME properties analysis from WCO and its standard are shown in Table 6. It shows that the FAME from WCO had a water content of 344 ppm, presumably appearing from palm oil's endocarp component. Besides that, the WCO has been in contact with other components during frying, which caused water's presence. Viscosity and density are the main factors for diesel fuel injection and efficient combustion (Ibeto et al., 2012). The higher the water content in the FAME, led the density (0.8711 Kg/L) and viscosity (4.872 cSt) were also higher. A heavy fraction in the methyl ester accompanies a higher distillation temperature and less distillate (92 mL) that is directly related to the relatively high carbon residue. This condition might inhibit the performance of the diesel engine. The FAME from WCO had the same color characteristics (1.5) as the pure diesel

fuel, which indicated that the FAME had similar good quality. In addition, the cetane index shows a reasonably good value (53.5) above the minimum standard of biodiesel (51). The higher the cetane index of fuel, the better the quality of the fuel as well as provided lower the delay period in the engines (Abdelhady et al., 2020). These results indicated that the FAME derived from WCO has the potential to be used as a blend to improve the quality of diesel fuel.

Table 6  
*Physicochemical properties of FAME from WCO*

| Properties                | Units                    | Results | FAME standard (EN 14214:2012) |
|---------------------------|--------------------------|---------|-------------------------------|
| Water content             | ppm                      | 344     | Max. 500                      |
| Density                   | Kg/L                     | 0.8711  | 0.860-0.900                   |
| Volume distillate         | mL                       | 92      | Min. 90                       |
| Kinematic viscosity, 40°C | mm <sup>2</sup> /s (cSt) | 4.872   | 3.5-5.0                       |
| Pour point                | °C                       | 6       | -                             |
| Color                     | -                        | 1.5     | -                             |
| Cetane index              | -                        | 53.5    | Min. 51                       |

### Effect of the FAME and Diesel Composition Blend

In this study, the FAME product derived from the WCO esterification was blended with diesel with various blends, namely B5, B10, B15, and B20, as previously mentioned. The B0 was referred to as the diesel without adding FAME, whereas the B100 was vice versa. The effect of FAME and diesel composition blend on water content and density are shown in Figure 9.

Analysis of water content using the ASTM D-6304 method showed that the FAME from WCO had a water content of 344 ppm (Figure 9). This value encounters the maximum limit of the biodiesel standard (500 ppm). The water content in methyl esters was quite high since biodiesel's density was close to water; thus, biodiesel was more easily bound to water. When the volume added of FAME to diesel fuel increased, the water content also increased (Figure 9). The lowest water content (314 ppm) was achieved by B5, whereas the highest water content (339 ppm) was achieved by B20. In this study, all blend compositions obtained a water content below 500 ppm, which met the criteria of the biodiesel standard. Most diesel engines are composed of metal, which is corrosive in the combustion chamber. High water content in the fuel could cause the hydrolysis of FAME and provoke the growth of microorganisms, which could block the flow in the combustion engine (Fregolente et al., 2012; Lin & Ma, 2020).

The density of diesel blended increased with the increasing volume of methyl ester added to diesel fuel (Figure 9). FAME contained oleic acid ( $C_{18}H_{34}O_2$ ), almost similar to diesel oil ( $C_{15}$ - $C_{20}$ ). When the methyl ester of oleic acid was mixed with diesel oil, it increased the length of the bond chain; thereby, the fraction in the blend increased. The density was directly proportional to the molecular weight. Thus, when the molecule's chain length increased, the blend's density also increased (Hajilar & Shafei, 2019). The density of the diesel composition blend ranged from 0.8507 to 0.8615 Kg/L, which indicated that the results follow the density of diesel fuel standards.

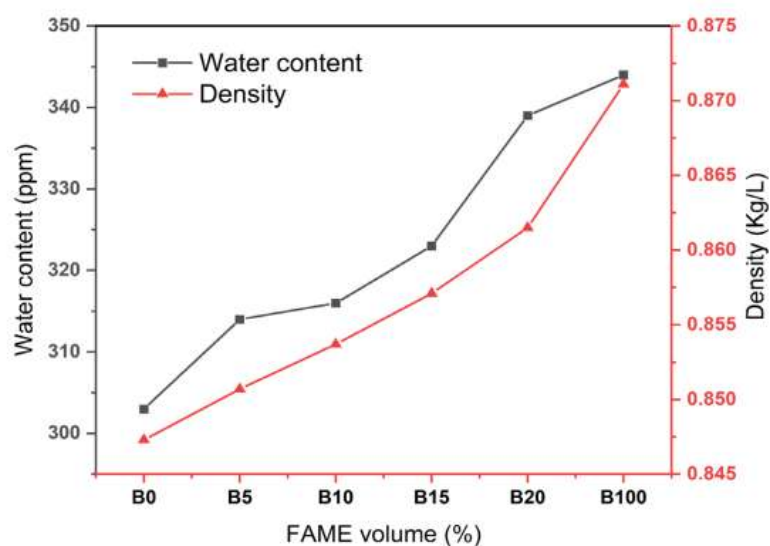


Figure 9. Effect of FAME and diesel composition blend on water content and density

The effect of FAME and diesel composition blend on distillate volume and viscosity are presented in Figure 10. The volume of distillate from the blend of FAME with diesel was lower than the FAME itself, which indicated that the weight fraction in FAME from WCO was relatively high. Similarly, the distillate volume decreased as the amount of FAME added to the diesel blend increased.

Viscosity reveals the lubricating properties of the fuel. Kinematic viscosity measurements using the ASTM D-445 method are conducted to determine the viscosity of fuel or the amount of internal resistance of a liquid to flow related to the supply of fuel consumption in the diesel engine combustion chamber. Kinematic viscosity is directly proportional to the length of the carbon chain and density. Subsequently, it can be seen from Figure 10 that the viscosity increased along with the increase of FAME volume to the diesel fuel. As viscosity is directly proportional to molecular weight, adding FAME to diesel would increase the carbon length chain, thereby increasing the viscosity. The higher

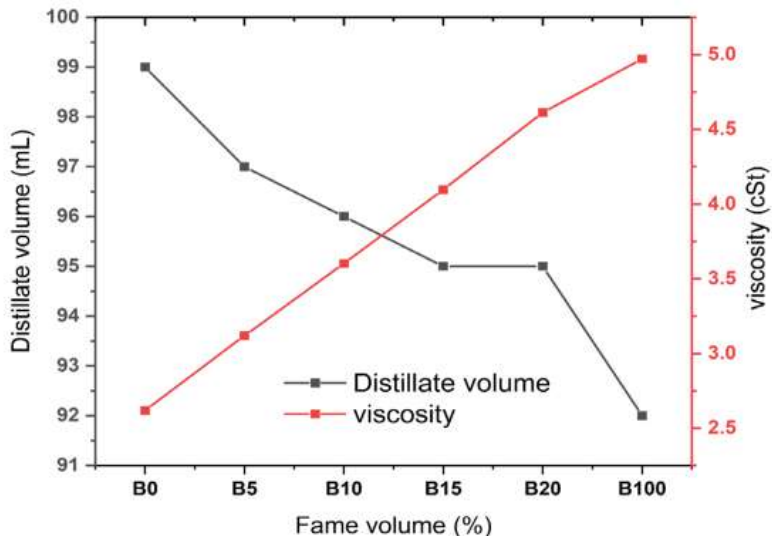


Figure 10. Effect of FAME and diesel composition blend on distillate volume and viscosity

the viscosity, the more difficult the combustion and the slower the piston work. All the blends were in accordance with diesel fuel standards, which corresponded to the engine's good atomization and complete combustion of biodiesel (Karmakar et al., 2018).

Kinematic viscosity measurements using the ASTM D-445 method are conducted to determine the viscosity of fuel or the amount of internal resistance of a liquid to flow related to the supply of fuel consumption in the diesel engine combustion chamber. Kinematic viscosity is directly proportional to the length of the carbon chain and density. Subsequently, it can be seen from Figure 10 that the viscosity increased along with the increase of FAME volume to the diesel fuel. As viscosity is directly proportional to molecular weight, adding FAME to diesel would increase the carbon length chain, thereby increasing the viscosity. The higher the viscosity, the more difficult the combustion and the slower the piston work. All the blends were in accordance with diesel fuel standards, which corresponded to the engine's good atomization and complete combustion of biodiesel (Karmakar et al., 2018).

The effect of FAME and diesel composition blend on color and pour point are shown in Figure 11. Color is a parameter that prevents the possibility of contamination by heavier fuels or water and other substances. This contamination affects the oil quality, resulting in operating failure and engine damage. The color observations results show a linear line on a scale of 1.5 (max. standard diesel = 3), which indicated that the FAME derived from WCO and their blends had a fairly good quality because they had an observation scale that was relatively close to diesel color (Figure 11).

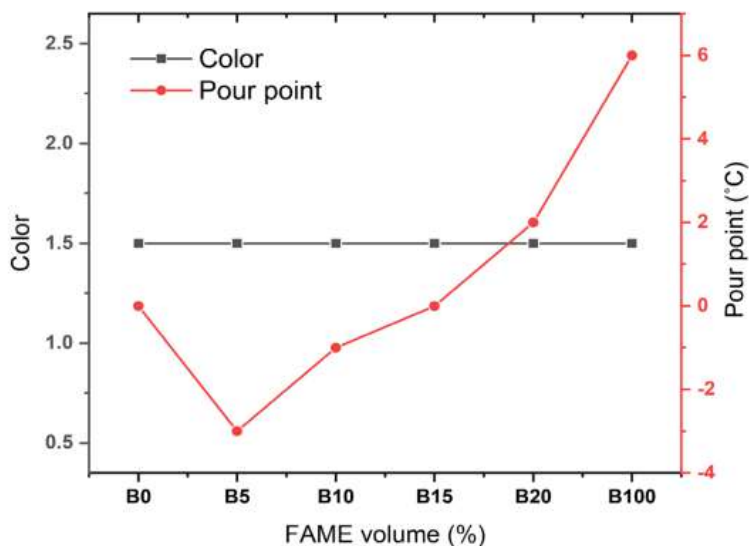


Figure 11. Effect of FAME and diesel composition blend on color and pour point

71

The pour point of FAME was quite high, at a temperature of 6°C, whereas diesel fuel was achieved at a temperature of 0°C (Figure 11). The pour points of B5 and B10 reached low temperatures of -3°C and -1°C, respectively, exceeding the pour point of pure diesel, whereas, in a blend of B15, the pour point was the same as the pure diesel, which was 0°C. Furthermore, the pour point of the B20 blend increased closer to FAME. The lower the pour point of the fuel, the better the engine's combustion quality because the fuel could still work to lubricate the engine at the lowest temperature. If the fuel is difficult to flow into the combustion chamber, it signifies that converting heat into motion energy by the piston is increasingly difficult. The type of oil and the content or components present in the oil influences the pour point quantity. In addition, the density, viscosity, and solubility of a gas in oil were also influenced.

The cetane index measurement was conducted to determine the ignition quality of diesel fuel. Diesel engines required a cetane number of roughly 50. The fuel cetane number was a volume percentage of cetane and alpha-methyl naphthalene, wherein cetane has better ignition qualities than alpha-methyl naphthalene. The cetane index was needed to prevent engine knocking. The higher the cetane index of diesel fuel, the better the combustion properties (Giakoumis & Sarakatsanis, 2018). The effect of FAME and diesel composition blend on the cetane index is presented in Figure 12.

The cetane index increases along with the amount of FAME added to the diesel blend (Figure 12). The cetane index of pure diesel was 48.5, whereas, after the addition of FAME (B20), the cetane index of the blend increased up to 51.2%. Furthermore, the blend of B10 and

B15 showed no significant difference in cetane index between the two blends. Generally, biodiesel has a higher cetane number than diesel, ranging from 46 to 70. The length of the hydrocarbon chain contains in the FAME caused the cetane number of biodiesel to be higher than diesel (Mishra et al., 2016). The increase of the cetane number from 48.5 to 51.2 would reduce carbon monoxide emissions by 5.27%. In terms of fuel consumption, increasing the cetane number would reduce both fuel engine consumption and engine noise (Rodríguez-Fernández et al., 2019). The results showed that the cetane index of all blends is in accordance with the standard for diesel, with a minimum cetane number of 48. The higher cetane number of biodiesel than diesel leads to better combustion properties of the engine.

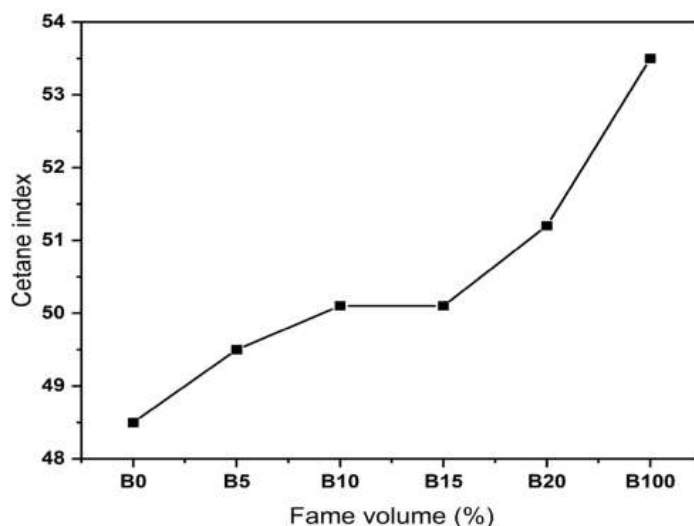


Figure 12. Effect of FAME and diesel composition blend on cetane index

## CONCLUSION

In this research, the free fatty acid (FFA) conversion from waste cooking oil (WCO) using montmorillonite-sulfonated carbon catalyst was conducted using response surface methodology (RSM) with a central composite design (CCD). The highest acidity of the catalyst was achieved up to 9.79 mmol/g by montmorillonite to sulfonated carbon 1:3 weight ratio catalyst. The montmorillonite-sulfonated carbon exhibited a higher surface area compared with montmorillonite. The optimum condition was obtained at a reaction temperature of 78.12°C, catalyst weight of 2.98 g, and reaction time of 118.27 with an FFA conversion of 74.101%. A sufficient statistical diagnostic revealed that the RSM-CCD quadratic model could accurately predict the FFA conversion from WCO using a montmorillonite-sulfonated carbon catalyst. The optimum condition for the blend of FAME

and diesel fuel was achieved at the composition of the blend of B20 and in good accordance with the FAME standard. The reusability of the catalyst at three consecutive runs showed that the catalyst had adequate stability but tended to decrease due to the leaching of the active site catalyst.

## ACKNOWLEDGEMENTS

The authors thank the Physical Chemistry laboratory and all members of the Biofuel Research Group, Faculty of Mathematics and Natural Science, Universitas Sriwijaya, for supporting research facilities.

## REFERENCES

- Abdelhady, H. H., Elazab, H. A., Ewais, E. M., Saber, M., & El-Deab, M. S. (2020). Efficient catalytic production of biodiesel using nano-sized sugar beet agro-industrial waste. *Fuel*, 261, Article 116481. <https://doi.org/10.1016/j.fuel.2019.116481>
- Akram, S., Mumtaz, M. W., Danish, M., Mukhtar, H., Irfan, A., Raza, S. A., Wang, Z., & Arshad, M. (2019). Impact of cerium oxide and cerium composite oxide as nano additives on the gaseous exhaust emission profile of waste cooking oil based biodiesel at full engine load conditions. *Renewable Energy*, 143, 898-905. <https://doi.org/10.1016/j.renene.2019.05.025>
- Ali, C. H., Asif, A. H., Iqbal, T., Qureshi, A. S., Kazmi, M. A., Yasin, S., Danish, M., & Mu, B. Z. (2018). Improved transesterification of waste cooking oil into biodiesel using calcined goat bone as a catalyst. *Energy Sources, Part A: Recovery, Utilization and Environmental Effects*, 40(9), 1076-1083. <https://doi.org/10.1080/15567036.2018.1469691>
- Almadani, E. A., Harun, F. W., Radzi, S. M., & Muhamad, S. K. (2018). Cu<sup>2+</sup> montmorillonite K10 clay catalyst as a green catalyst for production of stearic acid methyl ester: Optimization using response surface methodology (RSM). *Bulletin of Chemical Reaction Engineering & Catalysis*, 13(1), 187-195. <https://doi.org/10.9767/bcrec.13.1.1397.187-195>
- Al-Sakkari, E. G., Abdeldayem, O. M., El-Sheltawy, S. T., Abadir, M. F., Soliman, A., Rene, E. R., & Ismail, I. (2020). Esterification of high FFA content waste cooking oil through different techniques including the utilization of cement kiln dust as a heterogeneous catalyst: A comparative study. *Fuel*, 279, Article 118519. <https://doi.org/10.1016/j.fuel.2020.118519>
- Alshabanat, M., Al-Arrash, A., & Mekhamer, W. (2013). Polystyrene/montmorillonite nanocomposites: Study of the morphology and effects of sonication time on thermal stability. *Journal of Nanomaterials*, 2013, Article 650725. <https://doi.org/10.1155/2013/650725>
- Amaya, J., Suarez, N., Moreno, A., Moreno, S., & Molina, R. (2020). Mo or W catalysts promoted with Ni or Co supported on modified bentonite for decane hydroconversion. *New Journal of Chemistry*, 44(7), 2966-2979. <https://doi.org/10.1039/c9nj04878b>
- Anguebes-Franqueschi, F., Abatal, M., Bassam, A., Soberanis, M. A. E., Tzuc, O. M., Bucio-Galindo, L., Quiroz, A. V. C., Ucan, C. A. A., & Ramirez-Elias, M. A. (2018). Esterification optimization of crude African palm olein using response surface methodology and heterogeneous acid catalysis. *Energies*, 11(1), Article 157. <https://doi.org/10.3390/en11010157>

- Azman, N. S., Marliza, T. S., Asikin-Mijan, N., Hin, T. Y. Y., & Khairuddin, N. (2021). Production of biodiesel from waste cooking oil via deoxygenation using Ni-Mo/Ac catalyst. *Processes*, 9(5), Article 750. <https://doi.org/10.3390/pr9050750>
- Bahú, J., Hernandez, N., Bonon, A., Bonon, A. D. J., Mart, M., & Gregorio, J. (2017). Epoxy monomers obtained from castor oil using a toxicity-free catalytic system Related papers. *Journal of Molecular Catalysis A: Chemical*, 426, 550-556.
- Balajii, M., & Niju, S. (2021). Esterification optimization of underutilized Ceiba pentandra oil using response surface methodology. *Biofuels*, 12(5), 495-502. <https://doi.org/10.1080/17597269.2018.1496384>
- Banerjee, S., Sahani, S., & Sharma, Y. C. (2019). Process dynamic investigations and emission analyses of biodiesel produced using Sr-Ce mixed metal oxide heterogeneous catalyst. *Journal of Environmental Management*, 248, Article 109218. <https://doi.org/10.1016/j.jenvman.2019.06.119>
- Bastos, R. R. C., da Luz Corrêa, A. P., da Luz, P. T. S., da Rocha Filho, G. N., Zamian, J. R., & da Conceição, L. R. V. (2020). Optimization of biodiesel production using sulfonated carbon-based catalyst from an amazon agro-industrial waste. *Energy Conversion and Management*, 205, Article 112457. <https://doi.org/10.1016/j.enconman.2019.112457>
- Bayat, A., Baghdadi, M., & Bidhendi, G. N. (2018). Tailored magnetic nano-alumina as an efficient catalyst for transesterification of waste cooking oil: Optimization of biodiesel production using response surface methodology. *Energy Conversion and Management*, 177, 395-405. <https://doi.org/10.1016/j.enconman.2018.09.086>
- Boey, P. L., Ganesan, S., Maniam, G. P., Khairuddean, M., & Efendi, J. (2013). A new heterogeneous acid catalyst for esterification: Optimization using response surface methodology. *Energy Conversion and Management*, 65, 392-396. <https://doi.org/10.1016/j.enconman.2012.08.002>
- Boffito, D. C., Pirola, C., Galli, F., Di Michele, A., & Bianchi, C. L. (2013). Free fatty acids esterification of waste cooking oil and its mixtures with rapeseed oil and diesel. *Fuel*, 108, 612-619. <https://doi.org/10.1016/j.fuel.2012.10.069>
- Chandane, V. S., Rathod, A. P., Wasewar, K. L., & Jadhav, P. G. (2020). Response surface methodology and artificial neural networks for optimization of catalytic esterification of lactic acid. *Chemical Engineering and Technology*, 43(11), 2315-2324. <https://doi.org/10.1002/ceat.202000041>
- Chen, C., Chitose, A., Kusadokoro, M., Nie, H., Xu, W., Yang, F., & Yang, S. (2021). Sustainability and challenges in biodiesel production from waste cooking oil: An advanced bibliometric analysis. *Energy Reports*, 7, 4022-4034. <https://doi.org/10.1016/j.egyr.2021.06.084>
- Chen, S. Y., Attanatho, L., Chang, A., Laosombut, T., Nishi, M., Mochizuki, T., Takagi, H., Yang, C. M., Abe, Y., Toba, M., Chollacoop, N., & Yoshimura, Y. (2019). Profiling and catalytic upgrading of commercial palm oil-derived biodiesel fuels for high-blend fuels. *Catalysis Today*, 332, 122-131. <https://doi.org/10.1016/j.cattod.2018.05.039>
- Dawodu, F. A., Ayodele, O., Xin, J., Zhang, S., & Yan, D. (2014). Effective conversion of non-edible oil with high free fatty acid into biodiesel by sulphonated carbon catalyst. *Applied Energy*, 114, 819-826.
- de Oliveira, A. de N., de Lima, M. A. B., Pires, L. H. de O., da Silva, M. R., da Luz, P. T. S., Angélica, R. S., Filho, G. N. d. R., da Costa, C. E. F., Luque, R., & do Nascimento, L. A. S. (2019). Bentonites modified

with phosphomolybdic heteropolyacid (HPMo) for biowaste to biofuel production. *Materials*, 12(9), Article 1431. <https://doi.org/10.3390/ma12091431>

Dhawane, S. H., Kumar, T., & Halder, G. (2015). Central composite design approach towards optimization of flamboyant pods derived steam activated carbon for its use as heterogeneous catalyst in transesterification of *Hevea brasiliensis* oil. *Energy Conversion and Management*, 100, 277-287. <https://doi.org/10.1016/j.enconman.2015.04.083>

Dhawane, S. H., Kumar, T., & Halder, G. (2016). Biodiesel synthesis from *Hevea brasiliensis* oil employing carbon supported heterogeneous catalyst: Optimization by Taguchi method. *Renewable Energy*, 89, 506-514. <https://doi.org/10.1016/j.renene.2015.12.027>

Ding, J., Xia, Z., & Lu, J. (2012). Esterification and deacidification of a waste cooking oil (TAN 68.81 mg KOH/g) for biodiesel production. *Energies*, 5(8), 2683-2691. <https://doi.org/10.3390/en5082683>

Endut, A., Abdullah, S. H. Y. S., Hanapi, N. H. M., Hamid, S. H. A., Lananan, F., Kamarudin, M. K. A., Umar, R., Juahir, H., & Khatoon, H. (2017). Optimization of biodiesel production by solid acid catalyst derived from coconut shell via response surface methodology. *International Biodeterioration and Biodegradation*, 124, 250-257. <https://doi.org/10.1016/j.ibiod.2017.06.008>

Fadhil, A. B., Aziz, A. M., & Al-Tamer, M. H. (2016). Biodiesel production from *Silybum marianum* L. seed oil with high FFA content using sulfonated carbon catalyst for esterification and base catalyst for transesterification. *Energy Conversion and Management*, 108, 255-265. <https://doi.org/10.1016/j.enconman.2015.11.013>

Farabi, M. S. A., Ibrahim, M. L., Rashid, U., & Taufiq-Yap, Y. H. (2019). Esterification of palm fatty acid distillate using sulfonated carbon-based catalyst derived from palm kernel shell and bamboo. *Energy Conversion and Management*, 181, 562-570. <https://doi.org/10.1016/j.enconman.2018.12.033>

Fauziyah, M., Widiyastuti, W., & Setyawan, H. (2020). Sulfonated carbon aerogel derived from coir fiber as high performance solid acid catalyst for esterification. *Advanced Powder Technology*, 31(4), 1412-1419. <https://doi.org/10.1016/j.apt.2020.01.022>

Fawaz, E. G., Salam, D. A., & Daou, T. J. (2020). Esterification of linoleic acid using HZSM-5 zeolites with different Si/Al ratios. *Microporous and Mesoporous Materials*, 294, Article 109855. <https://doi.org/10.1016/j.micromeso.2019.109855>

Flores, K. P., Omega, J. L. O., Cabatingan, L. K., Go, A. W., Agapay, R. C., & Ju, Y. H. (2019). Simultaneously carbonized and sulfonated sugarcane bagasse as solid acid catalyst for the esterification of oleic acid with methanol. *Renewable Energy*, 130, 510-523. <https://doi.org/10.1016/j.renene.2018.06.093>

Fonseca, J. M., Spessato, L., Cazetta, A. L., Bedin, K. C., Melo, S. A. R., Souza, F. L., & Almeida, V. C. (2020). Optimization of sulfonation process for the development of carbon-based catalyst from crambe meal via response surface methodology. *Energy Conversion and Management*, 217, Article 112975. <https://doi.org/10.1016/j.enconman.2020.112975>

Fregolente, P. B. L., Fregolente, L. V., & Wolf Maciel, M. R. (2012). Water content in biodiesel, diesel, and biodiesel-diesel blends. *Journal of Chemical and Engineering Data*, 57(6), 1817-1821. <https://doi.org/10.1021/je300279c>

- Gan, S., Ng, H. K., Chan, P. H., & Leong, F. L. (2012). Heterogeneous free fatty acids esterification in waste cooking oil using ion-exchange resins. *Fuel Processing Technology*, 102, 67-72. <https://doi.org/10.1016/j.fuproc.2012.04.038>
- Giakoumis, E. G., & Sarakatsanis, C. K. (2018). Estimation of biodiesel cetane number, density, kinematic viscosity and heating values from its fatty acid weight composition. *Fuel*, 222, 574-585. <https://doi.org/10.1016/j.fuel.2018.02.187>
- Gupta, A. R., & Rathod, V. K. (2018). Waste cooking oil and waste chicken eggshells derived solid base catalyst for the biodiesel production: Optimization and kinetics. *Waste Management*, 79, 169-178. <https://doi.org/10.1016/j.wasman.2018.07.022>
- Hajilar, S., & Shafei, B. (2019). Thermal transport properties at interface of fatty acid esters enhanced with carbon-based nanoadditives. *International Journal of Heat and Mass Transfer*, 145, Article 118762. <https://doi.org/10.1016/j.ijheatmasstransfer.2019.118762>
- Hasanudin, H., Asri, W. R., Tampubolon, K., Riyant, F., Purwaningrum, W., & Wijaya, K. (2022). Dehydration isopropyl alcohol to diisopropyl ether over molybdenum phosphide pillared bentonite. *Pertanika Journal of Science & Technology*, 30(2), 1739-1754. <https://doi.org/10.47836/pjst.30.2.47>
- Hasanudin, H., Asri, W. R., Said, M., Hidayati, P. T., Purwaningrum, W., Novia, N., & Wijaya, K. (2022). Hydrocracking optimization of palm oil to bio-gasoline and bio-aviation fuels using molybdenum nitride-bentonite catalyst. *RSC Advances*, 12(26), 16431-16443. <https://doi.org/10.1039/D2RA02438A>
- Hasanudin, H., Putri, Q. U., Agustina, T. E., & Hadiah, F. (2022). Esterification of free fatty acid in palm oil mill effluent using sulfated carbon-zeolite composite catalyst. *Pertanika Journal of Science & Technology*, 30(1), 377-395. <https://doi.org/10.47836/pjst.30.1.21>
- Helmi, M., Tahvildari, K., Hemmati, A., Aberoomand Azar, P., & Safekordi, A. (2020). Phosphomolybdic acid/graphene oxide as novel green catalyst using for biodiesel production from waste cooking oil via electrolysis method: Optimization using with response surface methodology (RSM). *Fuel*, 287, Article 119528. <https://doi.org/10.1016/j.fuel.2020.119528>
- Ibeto, C. N., Okoye, C. O. B., & Ofoefule, A. U. (2012). Comparative study of the physicochemical characterization of some oils as potential feedstock for biodiesel production. *ISRN Renewable Energy*, 2012, 1-5. <https://doi.org/10.5402/2012/621518>
- Jamil, U., Khoja, A. H., Liaquat, R., Naqvi, S. R., Omar, W. N. N. W., & Amin, N. A. S. (2020). Copper and calcium-based metal organic framework (MOF) catalyst for biodiesel production from waste cooking oil: A process optimization study. *Energy Conversion and Management*, 215, Article 112934. <https://doi.org/10.1016/j.enconman.2020.112934>
- Jenie, S. N. A., Kristiani, A., Sudiyarmanto, Khaerudini, D. S., & Takeishi, K. (2020). Sulfonated magnetic nanobiochar as heterogeneous acid catalyst for esterification reaction. *Journal of Environmental Chemical Engineering*, 8(4), Article 103912. <https://doi.org/10.1016/j.jece.2020.103912>
- Kamaronzaman, M. F. F., Kahar, H., Hassan, N., Hanafi, M. F., & Sapawe, N. (2020a). Analysis of biodiesel product derived from waste cooking oil using fourier transform infrared spectroscopy. *Materials Today: Proceedings*, 31, 329-332. <https://doi.org/10.1016/j.matpr.2020.06.088>

Hasanudin Hasanudin, Wan Ryan Asri, Firda Rahmania Putri, Fahma Riyanti,  
Zainal Fanani, Addy Rachmat, Novia Novia and Tuty Emilia Agustina

- Kamaronzaman, M. F. F., Kahar, H., Hassan, N., Hanafi, M. F., & Sapawe, N. (2020b). Optimization of biodiesel production from waste cooking oil using eggshell catalyst. *Materials Today: Proceedings*, 31, 324-328. <https://doi.org/10.1016/j.matpr.2020.06.080>
- Karmakar, B., & Halder, G. (2021). Accelerated conversion of waste cooking oil into biodiesel by injecting 2-propanol and methanol under superheated conditions: A novel approach. *Energy Conversion and Management*, 247, Article 114733. <https://doi.org/10.1016/j.enconman.2021.114733>
- Karmakar, R., Kundu, K., & Rajor, A. (2018). Fuel properties and emission characteristics of biodiesel produced from unused algae grown in India. *Petroleum Science*, 15(2), 385-395. <https://doi.org/10.1007/s12182-017-0209-7>
- Kumar, S., Shamsuddin, M. R., Farabi, M. S. A., Saiman, M. I., Zainal, Z., & Taufiq-Yap, Y. H. (2020). Production of methyl esters from waste cooking oil and chicken fat oil via simultaneous esterification and transesterification using acid catalyst. *Energy Conversion and Management*, 226, Article 113366. <https://doi.org/10.1016/j.enconman.2020.113366>
- Kusumaningtyas, R. D., Prasetiawan, H., Putri, R. D. A., Triwibowo, B., Kurnita, S. C. F., Anggraeni, N. D., Veny, H., Hamzah, F., & Rodhi, M. N. M. (2021). Optimisation of free fatty acid removal in nyamplung seed oil (*Callophyllum inophyllum* L.) using response surface methodology analysis. *Pertanika Journal of Science and Technology*, 29(4), 2605-2623. <https://doi.org/10.47836/PJST.29.4.20>
- Lathiya, D. R., Bhatt, D. V., & Maheria, K. C. (2018). Synthesis of sulfonated carbon catalyst from waste orange peel for cost effective biodiesel production. *Bioresource Technology Reports*, 2, 69-76. <https://doi.org/10.1016/j.biteb.2018.04.007>
- Lin, C. Y., & Ma, L. (2020). Influences of water content in feedstock oil on burning characteristics of fatty acid methyl esters. *Processes*, 8(9), Article 1130. <https://doi.org/10.3390/PR8091130>
- Lin, J., Jiang, B., & Zhan, Y. (2018). Effect of pre-treatment of bentonite with sodium and calcium ions on phosphate adsorption onto zirconium-modified bentonite. *Journal of Environmental Management*, 217, 183-195. <https://doi.org/10.1016/j.jenvman.2018.03.079>
- Ma, Y., Wang, Q., Zheng, L., Gao, Z., Wang, Q., & Ma, Y. (2016). Mixed methanol/ethanol on transesterification of waste cooking oil using Mg/Al hydrotalcite catalyst. *Energy*, 107, 523-531. <https://doi.org/10.1016/j.energy.2016.04.066>
- Mahesh, S. E., Ramanathan, A., Begum, K. M. M. S., & Narayanan, A. (2015). Biodiesel production from waste cooking oil using KBr impregnated CaO as catalyst. *Energy Conversion and Management*, 91, 442-450. <https://doi.org/10.1016/j.enconman.2014.12.031>
- Mansir, N., Teo, S. H., Rabiu, I., & Taufiq-Yap, Y. H. (2018). Effective biodiesel synthesis from waste cooking oil and biomass residue solid green catalyst. *Chemical Engineering Journal*, 347, 137-144. <https://doi.org/10.1016/j.cej.2018.04.034>
- Mazubert, A., Aubin, J., Elgue, S., & Poux, M. (2014). Intensification of waste cooking oil transformation by transesterification and esterification reactions in oscillatory baffled and microstructured reactors for biodiesel production. *Green Processing and Synthesis*, 3(6), 419-429. <https://doi.org/10.1515/gps-2014-0057>

- Mishra, S., Anand, K., & Mehta, P. S. (2016). Predicting the cetane number of biodiesel fuels from their fatty acid methyl ester composition. *Energy and Fuels*, 30(12), 10425-10434. <https://doi.org/10.1021/acs.energyfuels.6b01343>
- Mulay, A., & Rathod, V. K. (2021). Microwave-assisted heterogeneous esterification of dibutyl maleate: Optimization using response surface methodology. *Chemical Data Collections*, 34, Article 100740. <https://doi.org/10.1016/j.cdc.2021.100740>
- Munir, M., Ahmad, M., Mubashir, M., Asif, S., Waseem, A., Mukhtar, A., Saqib, S., Munawaroh, H. S. H., Lam, M. K., Shiong Khoo, K., Bokhari, A., & Loke Show, P. (2021). A practical approach for synthesis of biodiesel via non-edible seeds oils using trimetallic based montmorillonite nano-catalyst. *Bioresouce Technology*, 328, Article 124859. <https://doi.org/10.1016/j.biortech.2021.124859>
- Narula, V., Khan, M. F., Negi, A., Kalra, S., Thakur, A., & Jain, S. (2017). Low temperature optimization of biodiesel production from algal oil using CaO and CaO/Al<sub>2</sub>O<sub>3</sub> as catalyst by the application of response surface methodology. *Energy*, 140, 879-884. <https://doi.org/10.1016/j.energy.2017.09.028>
- Nata, I. F., Putra, M. D., Irawan, C., & Lee, C. K. (2017). Catalytic performance of sulfonated carbon-based solid acid catalyst on esterification of waste cooking oil for biodiesel production. *Journal of Environmental Chemical Engineering*, 5(3), 2171-2175. <https://doi.org/10.1016/j.jece.2017.04.029>
- Ngaosuwan, K., Goodwin, J. G., & Prasertdham, P. (2016). A green sulfonated carbon-based catalyst derived from coffee residue for esterification. *Renewable Energy*, 86, 262-269. <https://doi.org/10.1016/j.renene.2015.08.010>
- Niu, S., Ning, Y., Lu, C., Han, K., Yu, H., & Zhou, Y. (2018). Esterification of oleic acid to produce biodiesel catalyzed by sulfonated activated carbon from bamboo. *Energy Conversion and Management*, 163(17923), 59-65. <https://doi.org/10.1016/j.enconman.2018.02.055>
- Noshadi, I., Amin, N. A. S., & Parnas, R. S. (2012). Continuous production of biodiesel from waste cooking oil in a reactive distillation column catalyzed by solid heteropolyacid: Optimization using response surface methodology (RSM). *Fuel*, 94, 156-164. <https://doi.org/10.1016/j.fuel.2011.10.018>
- Omidvarborna, H., Kumar, A., & Kim, D. (2016). Science of the total environment variation of diesel soot characteristics by different types and blends of biodiesel in a laboratory combustion chamber. *Science of the Total Environment*, 544, 450-459. <https://doi.org/10.1016/j.scitotenv.2015.11.076>
- Özbay, N., Oktar, N., & Tapan, N. A. (2008). Esterification of free fatty acids in waste cooking oils (WCO): Role of ion-exchange resins. *Fuel*, 87(10-11), 1789-1798. <https://doi.org/10.1016/j.fuel.2007.12.010>
- Palmonari, A., Cavallini, D., Sniffen, C. J., Fernandes, L., Holder, P., Fagioli, L., Fusaro, I., Biagi, G., Formigoni, A., & Mammi, L. (2020). Short communication: Characterization of molasses chemical composition. *Journal of Dairy Science*, 103(7), 6244-6249. <https://doi.org/10.3168/jds.2019-17644>
- Rabie, A. M., Mohammed, E. A., & Negm, N. A. (2018). Feasibility of modified bentonite as acidic heterogeneous catalyst in low temperature catalytic cracking process of biofuel production from nonedible vegetable oils. *Journal of Molecular Liquids*, 254(2018), 260-266. <https://doi.org/10.1016/j.molliq.2018.01.110>
- Rafati, A., Tahvildari, K., & Nozari, M. (2019). Production of biodiesel by electrolysis method from waste cooking oil using heterogeneous MgO-NaOH nano catalyst. *Energy Sources, Part A: Recovery, Utilization and Environmental Effects*, 41(9), 1062-1074. <https://doi.org/10.1080/15567036.2018.1539139>

- Rahimzadeh, H., Tabatabaei, M., Aghbashlo, M., Panahi, H. K. S., Rashidi, A., Goli, S. A. H., Mostafaei, M., Ardjomand, M., & Nizami, A. S. (2018). Potential of acid-activated bentonite and SO<sub>3</sub>H-functionalized MWCNTs for biodiesel production from residual olive oil under biorefinery scheme. *Frontiers in Energy Research*, 6, 1-10. <https://doi.org/10.3389/fenrg.2018.00137>
- Rocha, P. D., Oliveira, L. S., & Franca, A. S. (2019). Sulfonated activated carbon from corn cobs as heterogeneous catalysts for biodiesel production using microwave-assisted transesterification. *Renewable Energy*, 143, 1710-1716. <https://doi.org/10.1016/j.renene.2019.05.070>
- Rodríguez-Fernández, J., Hernández, J. J., Calle-Asensio, A., Ramos, Á., & Barba, J. (2019). Selection of blends of diesel fuel and advanced biofuels based on their physical and thermochemical properties. *Energies*, 12(11), Article 2034. <https://doi.org/10.3390/en12112034>
- Sahani, S., Roy, T., & Sharma, Y. C. (2020). Smart waste management of waste cooking oil for large scale high quality biodiesel production using Sr-Ti mixed metal oxide as solid catalyst: Optimization and E-metrics studies. *Waste Management*, 108, 189-201. <https://doi.org/10.1016/j.wasman.2020.04.036>
- Sari, E. P., Wijaya, K., Trisunaryanti, W., Syoufian, A., Hasanudin, H., & Saputri, W. D. (2021). The effective combination of zirconia superacid and zirconia-impregnated CaO in biodiesel manufacturing: Utilization of used coconut cooking oil (UCCO). *International Journal of Energy and Environmental Engineering*, 13, 967-978. <https://doi.org/10.1007/s40095-021-00439-4>
- Sharma, A., Kodgire, P., & Kachhwaha, S. S. (2019). Biodiesel production from waste cotton-seed cooking oil using microwave-assisted transesterification: Optimization and kinetic modeling. *Renewable and Sustainable Energy Reviews*, 116, Article 109394. <https://doi.org/10.1016/j.rser.2019.109394>
- Singh, V., Belova, L., Singh, B., & Sharma, Y. C. (2018). Biodiesel production using a novel heterogeneous catalyst, magnesium zirconate (Mg<sub>2</sub>Zr<sub>5</sub>O<sub>12</sub>): Process optimization through response surface methodology (RSM). *Energy Conversion and Management*, 174, 198-207. <https://doi.org/10.1016/j.enconman.2018.08.029>
- Soegiantoro, G. H., Chang, J., Rahmawati, P., Christiani, M. F., & Mufrodi, Z. (2019). Home-made ECO green biodiesel from chicken fat (CIAT) and waste cooking oil (pail). *Energy Procedia*, 158, 1105-1109. <https://doi.org/10.1016/j.egypro.2019.01.267>
- Sree, J. V., Chowdary, B. A., Kumar, K. S., Anbazhagan, M. P., & Subramanian, S. (2021). Optimization of the biodiesel production from waste cooking oil using homogeneous catalyst and heterogeneous catalysts. *Materials Today: Proceedings*, 46(10), 4900-4908. <https://doi.org/10.1016/j.matpr.2020.10.332>
- Suganuma, S., Nakajima, K., Kitano, M., & Hayashi, S. (2012). sp<sup>3</sup>-linked amorphous carbon with sulfonic acid groups as a heterogeneous acid catalyst. *ChemSusChem*, 5(9), 1841-1846. <https://doi.org/10.1002/cssc.201200010>
- Suresh, R., Antony, J. V., Vengalil, R., Kochimoolayil, G. E., & Joseph, R. (2017). Esterification of free fatty acids in non-edible oils using partially sulfonated polystyrene for biodiesel feedstock. *Industrial Crops and Products*, 95, 66-74. <https://doi.org/10.1016/j.indcrop.2016.09.060>
- Suwannasom, P., Tansupo, P., & Ruangviriyachai, C. (2016). A bone-based catalyst for biodiesel production from waste cooking oil. *Energy Sources, Part A: Recovery, Utilization and Environmental Effects*, 38(21), 3167-3173. <https://doi.org/10.1080/15567036.2015.1137998>

- Tan, Y. H., Abdullah, M. O., Nolasco-Hipolito, C., & Zauzi, N. S. A. (2017). Application of RSM and Taguchi methods for optimizing the transesterification of waste cooking oil catalyzed by solid ostrich and chicken-eggshell derived CaO. *Renewable Energy*, 114, 437-447. <https://doi.org/10.1016/j.renene.2017.07.024>
- Tang, Z. E., Lim, S., Pang, Y. L., Shuit, S. H., & Ong, H. C. (2020). Utilisation of biomass wastes based activated carbon supported heterogeneous acid catalyst for biodiesel production. *Renewable Energy*, 158, 91-102. <https://doi.org/10.1016/j.renene.2020.05.119>
- Wu, Z., Li, H., & Tu, D. (2015). Application of fourier transform infrared (FT-IR) spectroscopy combined with chemometrics for analysis of rapeseed oil adulterated with refining and purificating waste cooking oil. *Food Analytical Methods*, 8(10), 2581-2587. <https://doi.org/10.1007/s12161-015-0149-z>
- Xincheng, T., Niu, S., Zhao, S., Zhang, X., Li, X., Yu, H., Lu, C., & Han, K. (2019). Synthesis of sulfonated catalyst from bituminous coal to catalyze esterification for biodiesel production with promoted mechanism analysis. *Journal of Industrial and Engineering Chemistry*, 77, 432-440. <https://doi.org/10.1016/j.jiec.2019.05.008>
- Yahya, S., Wahab, S. K. M., & Harun, F. W. (2020). Optimization of biodiesel production from waste cooking oil using Fe-Montmorillonite K10 by response surface methodology. *Renewable Energy*, 157, 164-172. <https://doi.org/10.1016/j.renene.2020.04.149>
- Yuliana, M., Santoso, S. P., Soetaredjo, F. E., Ismadji, S., Ayucitra, A., Angkawijaya, A. E., Ju, Y. H., & Tran-Nguyen, P. L. (2020). A one-pot synthesis of biodiesel from leather tanning waste using supercritical ethanol: Process optimization. *Biomass and Bioenergy*, 142, Article 105761. <https://doi.org/10.1016/j.biombioe.2020.105761>
- Zhang, B., Gao, M., Geng, J., Cheng, Y., Wang, X., Wu, C., Wang, Q., Liu, S., & Cheung, S. M. (2021). Catalytic performance and deactivation mechanism of a one-step sulfonated carbon-based solid-acid catalyst in an esterification reaction. *Renewable Energy*, 164, 824-832. <https://doi.org/10.1016/j.renene.2020.09.076>
- Zhang, H., Gao, J., Zhao, Z., Chen, G. Z., Wu, T., & He, F. (2016). Esterification of fatty acids from waste cooking oil to biodiesel over a sulfonated resin/PVA composite. *Catalysis Science and Technology*, 6(14), 5590-5598. <https://doi.org/10.1039/c5cy02133b>
- Zhang, M., Sun, A., Meng, Y., Wang, L., Jiang, H., & Li, G. (2015). High activity ordered mesoporous carbon-based solid acid catalyst for the esterification of free fatty acids. *Microporous and Mesoporous Materials*, 204, 210-217. <https://doi.org/10.1016/j.micromeso.2014.11.027>
- Zik, N. A. F. A., Sulaiman, S., & Jamal, P. (2020). Biodiesel production from waste cooking oil using calcium oxide/nanocrystal cellulose/polyvinyl alcohol catalyst in a packed bed reactor. *Renewable Energy*, 155, 267-277. <https://doi.org/10.1016/j.renene.2020.03.144>



---

## ORIGINALITY REPORT

---

# 18%

SIMILARITY INDEX

---

### PRIMARY SOURCES

---

- 1 [biodesealeducation.org](https://biodesealeducation.org) Internet 86 words — 1 %
- 2 Qodria Utami Putri, Hasanudin Hasanudin, Wan Ryan Asri, Ady Mara, Roni Maryana, Saharman Gea, Karna Wijaya. "Production of levulinic acid from glucose using nickel phosphate-silica catalyst", Reaction Kinetics, Mechanisms and Catalysis, 2022  
Crossref 56 words — 1 %
- 3 Hasanudin Hasanudin, Wan Ryan Asri, Muhammad Said, Putri Tamara Hidayati, Widia Purwaningrum, Novia Novia, Karna Wijaya. "Hydrocracking optimization of palm oil to bio-gasoline and bio-aviation fuels using molybdenum nitride-bentonite catalyst", RSC Advances, 2022  
Crossref 49 words — 1 %
- 4 [studentsrepo.um.edu.my](https://studentsrepo.um.edu.my) Internet 47 words — 1 %
- 5 [www.tandfonline.com](https://www.tandfonline.com) Internet 39 words — < 1 %
- 6 Hasanudin Hasanudin, Wan Ryan Asri, Lepa Husnia, Zainal Fanani et al. "Catalytic dehydration of 2-propanol over nickel phosphide immobilized on natural bentonite", Reaction Kinetics, Mechanisms and Catalysis, 2023  
Crossref 37 words — < 1 %

- 7 Maryam Helmi, Kambiz Tahvildari, Alireza Hemmati, Parviz Aberoomand azar, Aliakbar Safekordi. "Phosphomolybdic acid/graphene oxide as novel green catalyst using for biodiesel production from waste cooking oil via electrolysis method: Optimization using with response surface methodology (RSM)", Fuel, 2020  
Crossref
- 8 eprints.usm.my Internet 29 words – < 1 %
- 9 Gerhard Knothe. "'Designer' Biodiesel: Optimizing Fatty Ester Composition to Improve Fuel Properties", Energy & Fuels, 2008  
Crossref
- 10 Wendy Mateo, Hanwu Lei, Elmar Villota, Moriko Qian, Yunfeng Zhao, Erguang Huo, Qingfa Zhang, Xiaona Lin, Chenxi Wang. "One-step synthesis of biomass-based sulfonated carbon catalyst by direct carbonization-sulfonation for organosolv delignification", Bioresource Technology, 2021  
Crossref
- 11 Ibrahim M. Lokman, Umer Rashid, Yun Hin Taufiq-Yap, Robiah Yunus. "Methyl ester production from palm fatty acid distillate using sulfonated glucose-derived acid catalyst", Renewable Energy, 2015  
Crossref
- 12 Usman Idris Nda-Umar, Ramli Irmawati, Ernee Noryana Muhamad, Norsahida Azri et al. "Organosulfonic acid-functionalized biomass-derived carbon as a catalyst for glycerol acetylation and optimization studies via response surface methodology", Journal of the Taiwan Institute of Chemical Engineers, 2021  
Crossref
- 13 psasir.upm.edu.my Internet

24 words — < 1%

- 14 [www.mdpi.com](http://www.mdpi.com)  
Internet

24 words — < 1%

- 15 Ray Vern Quah, Yie Hua Tan, N.M. Mubarak, Jibrail Kansedo, Mohammad Khalid, E.C. Abdullah, Mohammad Omar Abdullah. "Magnetic biochar derived from waste palm kernel shell for biodiesel production via sulfonation", Waste Management, 2020  
[Crossref](#)

23 words — < 1%

- 16 Hellna Tehubijuluw, Riki Subagyo, Maulil Fatma Yulita, Reva Edra Nugraha et al. "Utilization of red mud waste into mesoporous ZSM-5 for methylene blue adsorption-desorption studies", Environmental Science and Pollution Research, 2021  
[Crossref](#)

22 words — < 1%

- 17 Liu Chunying, Liu Yunqi, Li Wangliang, Cui Min, Liu Chenguang. "Hydrogenation of Naphthalene on HY/MCM-41 Composite Supported Sulfided Ni-Mo Catalysts", Petroleum Science and Technology, 2006  
[Crossref](#)

22 words — < 1%

- 18 Serly J. Sekewael. "Determination of Surface Acidity on The Natural and Synthetic Montmorillonite Clays by Titration Method", Indo. J. Chem. Res, 2021  
[Crossref](#)

20 words — < 1%

- 19 [rmiq.org](http://rmiq.org)  
Internet

19 words — < 1%

- 20 "Green Diesel: An Alternative to Biodiesel and Petrodiesel", Springer Science and Business Media LLC, 2022  
[Crossref](#)

18 words — < 1%

- 21 Ratanaporn Leesing, Siraprapha Siwina, Khanittha Fiala. "Yeast-based biodiesel production using sulfonated carbon-based solid acid catalyst by an integrated biorefinery of durian peel waste", Renewable Energy, 2021  
Crossref
- 17 words – < 1%
- 22 Joshua Iseoluwa Orege, Olayinka Oderinde, Ghebretenesa Aron Kifle, Adeola Ahmed Ibikunle et al. "Recent advances in heterogeneous catalysis for green biodiesel production by transesterification", Energy Conversion and Management, 2022  
Crossref
- 16 words – < 1%
- 23 Remi Ayu Pratika, Karna Wijaya, Wega Trisunaryanti. "Hydrothermal treatment of SO<sub>4</sub>/TiO<sub>2</sub> and TiO<sub>2</sub>/CaO as heterogeneous catalysts for the conversion of Jatropha oil into biodiesel", Journal of Environmental Chemical Engineering, 2021  
Crossref
- 16 words – < 1%
- 24 Semakula Maroa, Freddie Inambao. "Biodiesel, Combustion, Performance and Emissions Characteristics", Springer Science and Business Media LLC, 2020  
Crossref
- 16 words – < 1%
- 25 research.wsulibs.wsu.edu:8080 Internet
- 16 words – < 1%
- 26 Nam Nghiep Tran, Marina Tišma, Sandra Budžaki, Edward J. McMurchie et al. "Production of Biodiesel from Recycled Grease Trap Waste: A Review", Industrial & Engineering Chemistry Research, 2021  
Crossref
- 15 words – < 1%
- 27 ebin.pub Internet
- 15 words – < 1%

- 28 etd.aau.edu.et Internet 15 words – < 1%
- 29 par.nsf.gov Internet 15 words – < 1%
- 30 D.R. Lathiya, D.V. Bhatt, K.C. Maheria. "Synthesis of sulfonated carbon catalyst from waste orange peel for cost effective biodiesel production", Bioresource Technology Reports, 2018  
Crossref 13 words – < 1%
- 31 Fazril Ideris, Abd Halim Shamsuddin, Saifuddin Nomanbhay, Fitranto Kusumo et al. "Optimization of ultrasound-assisted oil extraction from Canarium odontophyllum kernel as a novel biodiesel feedstock", Journal of Cleaner Production, 2020  
Crossref 13 words – < 1%
- 32 Soroush Soltani, Umer Rashid, Imededdine Arbi Nehdi, Saud Ibrahim Al-Resayes, Ala'a H. Al-Muhtaseb. "Sulfonated mesoporous zinc aluminate catalyst for biodiesel production from high free fatty acid feedstock using microwave heating system", Journal of the Taiwan Institute of Chemical Engineers, 2017  
Crossref 13 words – < 1%
- 33 T. Pholsawang, Varinrumpai Seithtanabutara, P. Keawkannetra, Tanakorn Wongwuttanasatian. "Dual Frequency Ultrasound-Assisted Esterification of Palm Empty Fruit Bunch Oil with Zeolite Heterogeneous Acid Catalyst", Key Engineering Materials, 2022  
Crossref 13 words – < 1%
- 34 Unza Jamil, Asif Husain Khoja, Rabia Liaquat, Salman Raza Naqvi, Wan Nor Nadyaini Wan Omar, Nor Aishah Saidina Amin. "Copper and calcium-based metal organic framework (MOF) catalyst for biodiesel 13 words – < 1%

- 35 E. W. Landen. "COMBUSTION STUDIES of the DIESEL ENGINE", SAE International, 1946 12 words — < 1%  
Crossref
- 36 Hadi Rahimzadeh, Meisam Tabatabaei, Mortaza Aghbashlo, Hamed Kazemi Shariat Panahi et al. "Potential of Acid-Activated Bentonite and SO3H-Functionalized MWCNTs for Biodiesel Production From Residual Olive Oil Under Biorefinery Scheme", Frontiers in Energy Research, 2018 12 words — < 1%  
Crossref
- 37 Sirada Patthawaro, Chewapat Saejung. "Production of single cell protein from manure as animal feed by using photosynthetic bacteria", MicrobiologyOpen, 2019 12 words — < 1%  
Crossref
- 38 S. Swetha, Mostafa A. Abdel-Maksoud, Mohammad K. Okla, B. Janani, Turki M. Dawoud, Mohamed A. El-Tayeb, S. Sudheer Khan. "Triple-mechanism driven Fe-doped n-n hetero-architecture of Pr<sub>6</sub>O<sub>11</sub>-MoO<sub>3</sub> decorated g-C<sub>3</sub>N<sub>4</sub> for doxycycline degradation and bacterial photoinactivation", Chemical Engineering Journal, 2023 11 words — < 1%  
Crossref
- 39 Satheesh, K., P. E. JagadeeshBabu, and M. B. Saidutta. "Two-step Biodiesel Production and its Kinetics Studies Using Indion-190/AmberliteIRA-900 from Waste Cooking Oil", Energy Sources Part A Recovery Utilization and Environmental Effects, 2015. 11 words — < 1%  
Crossref
- 40 Shamshad Ahmad, Shalini Chaudhary, Vinayak V. Pathak, Richa Kothari, Vineet V. Tyagi. 11 words — < 1%

"Optimization of direct transesterification of Chlorella pyrenoidosa catalyzed by waste egg shell based heterogenous nano - CaO catalyst", Renewable Energy, 2020

Crossref

- 41 journal.unimma.ac.id Internet 11 words – < 1%
- 42 "Horizons in Bioprocess Engineering", Springer Science and Business Media LLC, 2019 10 words – < 1%  
Crossref
- 43 Ester Gutierrez-Acebo, Charles Leroux, Céline Chizallet, Yves Schuurman, Christophe Bouchy. "Metal/Acid Bifunctional Catalysis and Intimacy Criterion for Ethylcyclohexane Hydroconversion: When Proximity Does Not Matter", ACS Catalysis, 2018 10 words – < 1%  
Crossref
- 44 Falowo, Ojumu, Pereao, Betiku. "Sustainable Biodiesel Synthesis from Honne-Rubber-Neem Oil Blend with a Novel Mesoporous Base Catalyst Synthesized from a Mixture of Three Agrowastes", Catalysts, 2020 10 words – < 1%  
Crossref
- 45 Fang Li, Hongfang Ma, Weiyong Ying. "Application of Response Surface Methodology and Central Composite Rotatable Design for Modeling and Optimization of Catalyst Compositions in Ethanol Synthesis via CO Hydrogenation", International Journal of Chemical Reactor Engineering, 2014 10 words – < 1%  
Crossref
- 46 Ghazaleh Farokhi, Majid Saidi. "Catalytic Activity of Bimetallic Spinel Magnetic Catalysts (NiZnFe<sub>2</sub>O<sub>4</sub>, CoZnFe<sub>2</sub>O<sub>4</sub> and CuZnFe<sub>2</sub>O<sub>4</sub>) in Biodiesel Production process from Neem Oil: Process Evaluation and Optimization", Chemical Engineering and Processing - Process Intensification, 2022 10 words – < 1%

- 47 Rayanne O. Araujo, Vanuza O. Santos, Flaviana C. P. Ribeiro, Jamal da S. Chaar, Newton P. S. Falcão, Luiz K. C. de Souza. "One-step synthesis of a heterogeneous catalyst by the hydrothermal carbonization of acai seed", Reaction Kinetics, Mechanisms and Catalysis, 2021  
Crossref
- 10 words — < 1 %
- 48 Thi Tuong Vi Tran, Suwadee Kongparakul, Prasert Reubroycharoen, Guoqing Guan, Manh Huan Nguyen, Narong Chanlek, Chanatip Samart. "Production of furan based biofuel with an environmental benign carbon catalyst", Environmental Progress & Sustainable Energy, 2017  
Crossref
- 10 words — < 1 %
- 49 Vishal Narula, Mohd. Fazil Khan, Ankit Negi, Shashvat Kalra, Aman Thakur, Siddharth Jain. "Low Temperature Optimization of Biodiesel Production from Algal oil using CaO and CaO/Al<sub>2</sub>O<sub>3</sub> as catalyst by the application of Response Surface Methodology", Energy, 2017  
Crossref
- 10 words — < 1 %
- 50 www.degruyter.com Internet
- 10 words — < 1 %
- 51 "Waste-to-Energy", Springer Science and Business Media LLC, 2022  
Crossref
- 9 words — < 1 %
- 52 Carla V.R. Moura, Wiury C. Abreu, Edmilson M. Moura, Jean C.S. Costa. "CaO derived from waste shell materials as catalysts in synthesis of biodiesel", Elsevier BV, 2022  
Crossref
- 9 words — < 1 %
- 53 Chao Chen, Shaokang Qu, Mengli Guo, Jie Lu, Weiming Yi, Ransheng Liu, Jincheng Ding. "Waste limescale derived recyclable catalyst and soybean dregs oil
- 9 words — < 1 %

for biodiesel production: Analysis and optimization", Process Safety and Environmental Protection, 2021

Crossref

- 54 Hasanudin Hasanudin, Wan Ryan Asri, Indah Sari Zulaikha, Cik Ayu et al. "Hydrocracking of crude palm oil to a biofuel using zirconium nitride and zirconium phosphide-modified bentonite", RSC Advances, 2022  
Crossref
- 9 words — < 1%
- 55 Lingling Ma, Enmin Lv, Lixiong Du, Ying Han, Jie Lu, Jincheng Ding. "A flow-through tubular catalytic membrane reactor using zirconium sulfate tetrahydrate-impregnated carbon membranes for acidified oil esterification", Journal of the Energy Institute, 2017  
Crossref
- 9 words — < 1%
- 56 N.A.F.A. Zik, S. Sulaiman, P. Jamal. "Biodiesel production from waste cooking oil using calcium oxide/nanocrystal cellulose/polyvinyl alcohol catalyst in a packed bed reactor", Renewable Energy, 2020  
Crossref
- 9 words — < 1%
- 57 Shangeetha Ganesan, Hao Sen Siow, Akintomiwa O. Esan, Sivajothi Nadarajah, Nur Liyana Abdul Manaff. "Introduction", Elsevier BV, 2022  
Crossref
- 9 words — < 1%
- 58 Sumit H. Dhawane, Tarkeshwar Kumar, Gopinath Halder. "Parametric effects and optimization on synthesis of iron (II) doped carbonaceous catalyst for the production of biodiesel", Energy Conversion and Management, 2016  
Crossref
- 9 words — < 1%
- 59 Upender Kumar, Pardeep Gupta. "Modeling and optimization of novel biodiesel production from non-edible oil with musa balbisiana root using hybrid response surface methodology along with african buffalo
- 9 words — < 1%

- 60 Wenlei Xie, Cong Qi, Hongyan Wang, Yawei Liu. "Phenylsulfonic acid functionalized mesoporous SBA-15 silica: A heterogeneous catalyst for removal of free fatty acids in vegetable oil", Fuel Processing Technology, 2014  
Crossref 9 words — < 1 %
- 61 kanazawa-u.repo.nii.ac.jp Internet 9 words — < 1 %
- 62 komunikacie.uniza.sk Internet 9 words — < 1 %
- 63 www.frontiersin.org Internet 9 words — < 1 %
- 64 "Bioresource Utilization and Bioprocess", Springer Science and Business Media LLC, 2020 Crossref 8 words — < 1 %
- 65 D. Yogaraj, S. Jaichandar. "An assessment of various nanoadditives and tribocorrosion with waste cooking biodiesel fueled in a diesel engine", Transactions of the Canadian Society for Mechanical Engineering, 2022 Crossref 8 words — < 1 %
- 66 Debasis Borah, Harshajit Nath, Hemaprobonha Saikia. "Modification of bentonite clay & its applications: a review", Reviews in Inorganic Chemistry, 2021 Crossref 8 words — < 1 %
- 67 Gaoqiang Zhang, Wenlei Xie. "ZrMo oxides supported catalyst with hierarchical porous structure for cleaner and sustainable production of biodiesel using acidic oils as feedstocks", Journal of Cleaner Production, 2022 Crossref 8 words — < 1 %

- 68 Hasanudin Hasanudin, Wan Ryan Asri, Lola Andini, Fahma Riyanti, Ady Mara, Fitri Hadiah, Zainal Fanani. "Enhanced Isopropyl Alcohol Conversion over Acidic Nickel Phosphate-Supported Zeolite Catalysts", ACS Omega, 2022  
Crossref 8 words – < 1%
- 69 Hewei Yu, Shengli Niu, Chunmei Lu, Wei Wei, Xingyu Zhang. "Biodiesel synthesis by transesterification using coal-based solid acid catalyst", IOP Conference Series: Earth and Environmental Science, 2021  
Crossref 8 words – < 1%
- 70 I. Istadi, Teguh Riyanto, Elok Khofiyanida, Luqman Buchori et al. "Low-oxygenated biofuels production from palm oil through hydrocracking process using the enhanced Spent RFCC catalysts", Bioresource Technology Reports, 2021  
Crossref 8 words – < 1%
- 71 Mar'atul Fauziyah, Widiyastuti Widiyastuti, Heru Setyawan. "Sulfonated carbon aerogel derived from coir fiber as high performance solid acid catalyst for esterification", Advanced Powder Technology, 2020  
Crossref 8 words – < 1%
- 72 Matheus Cavali, Nelson Libardi Junior, Julia Dutra de Sena, Adenise Lorenci Woiciechowski et al. "A review on hydrothermal carbonization of potential biomass wastes, characterization and environmental applications of hydrochar, and biorefinery perspectives of the process", Science of The Total Environment, 2023  
Crossref 8 words – < 1%
- 73 Niran Daimary, Khalifa S.H. Eldiehy, Neelam Bora, Pankaj Boruah et al. "Towards integrated sustainable biofuel and chemical production: An application of banana pseudostem ash in the production of biodiesel and recovery of lignin from bamboo leaves", Chemosphere, 2023  
8 words – < 1%

- 74 Noor Azira Abdul Razak, Nurul-Asikin Mijan, Yun Hin Taufiq-Yap, Darfizzi Derawi. "Production of green diesel via hydrogen-free and solventless deoxygenation reaction of waste cooking oil", Journal of Cleaner Production, 2022  
Crossref
- 8 words – < 1%
- 75 S. Sudalai, Pothiappan Vairaprakash, M.G. Devanesan, A. Arumugam. "Sustainable biodiesel production from Madhuca indica oil using a functionalized industrial waste as a catalyst: Ready to scale-up approach", Industrial Crops and Products, 2023  
Crossref
- 8 words – < 1%
- 76 Shatesh Kumar Sangar, Chin Sook Lan, S.M. Razali, M.S. Ahmad Farabi, Yun Hin Taufiq-Yap. "Methyl ester production from palm fatty acid distillate (PFAD) using sulfonated cow dung-derived carbon-based solid acid catalyst", Energy Conversion and Management, 2019  
Crossref
- 8 words – < 1%
- 77 Siri Fung Basumatary, Khemnath Patir, Bipul Das, Pankaj Saikia et al. "Production of renewable biodiesel using metal organic frameworks based materials as efficient heterogeneous catalysts", Journal of Cleaner Production, 2022  
Crossref
- 8 words – < 1%
- 78 Steven Lim, Chin Yi Yap, Yean Ling Pang, Kam Huei Wong. "Biodiesel synthesis from oil palm empty fruit bunch biochar derived heterogeneous solid catalyst using 4-benzenediazonium sulfonate", Journal of Hazardous Materials, 2019  
Crossref
- 8 words – < 1%
- 79 Wan - Ying Wong, Steven Lim, Yean - Ling Pang, Wei - Hsin Chen, Man - Kee Lam, Inn - Shi Tan.  
Crossref
- 8 words – < 1%

"Synthesis of glycerol - free fatty acid methyl ester using interesterification reaction based on solid acid carbon catalyst derived from low - cost biomass wastes", International Journal of Energy Research, 2020

Crossref

- 80 Yie Hua Tan, Mohammad Omar Abdullah, Cirilo Nolasco-Hipolito, Nur Syuhada Ahmad Zauzi. 8 words – < 1%  
"Application of RSM and Taguchi methods for optimizing the transesterification of waste cooking oil catalyzed by solid ostrich and chicken-eggshell derived CaO", Renewable Energy, 2017  
Crossref
- 81 eprints.utar.edu.my 8 words – < 1%  
Internet
- 82 espace.curtin.edu.au 8 words – < 1%  
Internet
- 83 journals-jd.upm.edu.my 8 words – < 1%  
Internet
- 84 ouci.dntb.gov.ua 8 words – < 1%  
Internet
- 85 www.hindawi.com 8 words – < 1%  
Internet
- 86 www.pertanika2.upm.edu.my 8 words – < 1%  
Internet
- 87 www.pub.iapchem.org 8 words – < 1%  
Internet
- 88 "Biodiesel Production", Wiley, 2022 7 words – < 1%  
Crossref
- 89 Rose Fadzilah Abdullah, Umer Rashid, Balkis Hazmi, Mohd Lokman Ibrahim, Toshiki Tsubota, 7 words – < 1%

Fahad A. Alharthi. "Potential heterogeneous nano-catalyst via integrating hydrothermal carbonization for biodiesel production using waste cooking oil", Chemosphere, 2021

Crossref

- 90 Vikas Sharma, Abul Kalam Hossain, Ganesh Duraisamy, Murugan Vijay. "Transesterification of Pyrolysed Castor Seed Oil in the Presence of CaCu(OCH<sub>3</sub>)<sub>2</sub> Catalyst", Energies, 2021 7 words — < 1 %  
Crossref
- 91 "Trends in Manufacturing and Engineering Management", Springer Science and Business Media LLC, 2021 6 words — < 1 %  
Crossref
- 92 Anton Alvarez-Majmudov, Sandeep Badoga, Jinwen Chen, Jacques Monnier, Yi Zhang. "Co-Processing of Deoxygenated Pyrolysis Bio-Oil with Vacuum Gas Oil through Hydrocracking", Energy & Fuels, 2021 6 words — < 1 %  
Crossref
- 93 B. Devaraj Naik, M. Udayakumar. "Optimization and characterization studies on the production of bio-diesel from WSO using carbon catalyst derived from coconut meal residue", Energy Sources, Part A: Recovery, Utilization, and Environmental Effects, 2019 6 words — < 1 %  
Crossref
- 94 Farrukh Jamil, Lamya Al-Haj, Ala'a H. Al-Muhtaseb, Mohab A. Al-Hinai, Mahad Baawain, Umer Rashid, Mohammad N.M. Ahmad. "Current scenario of catalysts for biodiesel production: a critical review", Reviews in Chemical Engineering, 2018 6 words — < 1 %  
Crossref
- 95 Jhessica M. Fonseca, Lucas Spessato, André L. Cazetta, Camila da Silva, Vitor de C. Almeida. "Sulfonated carbon: synthesis, properties and production of 6 words — < 1 %

biodiesel", Chemical Engineering and Processing - Process Intensification, 2022

Crossref

- 96 Mei Yin Ong, Kit Wayne Chew, Pau Loke Show, Saifuddin Nomanbhay. "Optimization and kinetic study of non-catalytic transesterification of palm oil under subcritical condition using microwave technology", Energy Conversion and Management, 2019

Crossref

- 97 Shatesh Kumar, Mohd Razali Shamsuddin, M.S Ahmad Farabi, Mohd Izham Saiman, Zulkarnain Zainal, Yun Hin Taufiq-Yap. "Production of methyl esters from waste cooking oil and chicken fat oil via simultaneous esterification and transesterification using acid catalyst", Energy Conversion and Management, 2020

Crossref

- 98 Soo-Young No. "Application of Liquid Biofuels to Internal Combustion Engines", Springer Science and Business Media LLC, 2019

Crossref

- 99 Ying Li, Xincheng Tang, Shengli Niu, Yongzheng Wang, Kuihua Han, Chunmei Lu. "Synthesis of the zirconium dioxide activated carbon-based heterogeneous acid catalyst to catalyze esterification for biodiesel production with molecular simulation", Biomass Conversion and Biorefinery, 2021

Crossref

EXCLUDE QUOTES

OFF

EXCLUDE BIBLIOGRAPHY

ON

EXCLUDE SOURCES

OFF

EXCLUDE MATCHES

OFF